Transient fluvial incision in the headwaters of the Yellow River, northeastern Tibet, China

Nathan Harkins,[1] Eric Kirby,[1] Arjun Heimsath,[2] Ruth Robinson,[3] and Uwe Reiser[4]

Received 9 May 2006; revised 13 April 2007; accepted 29 June 2007; published 22 September 2007.

[1] We utilize topographic analysis of channel profiles combined with field measurements of erosion rates to explore the distribution of channel incision in the Anyemaqen Shan, a broad mountainous region in the northeastern Tibetan plateau. Tributary channels to the Yellow River display systematic downstream increases in channel gradient associated with convex upward longitudinal profiles. Steep lower reaches of channels are associated with rapid (>1 m/ka) incision rates along the Yellow River, while upstream reaches are associated with relatively slow (0.05–0.1 m/ka) erosion of soil-mantled uplands. Covariance between erosion rates and channel steepness indices suggest that channels are adjusted to match long-wavelength differential rock uplift across the range. Geologic constraints indicate that rapid incision downstream of the range is associated with excavation of basin fill driven by changes in relative base level farther downstream. The upstream limit of this wave of transient incision is marked by a series of knickpoints that are found at nearly the same elevation throughout the watershed, consistent with knickpoint migration as a kinematic, rather than diffusional, wave. Tributary channel gradients downstream of knickpoints, however, display a progressive adjustment to increased incision rates that may reflect the influence of increased sediment flux. Comparison of observed channel profiles to a stream power model of fluvial behavior reveals that the rate of knickpoint propagation can only be explained if the erosional efficiency coefficient (K) increases during incision. Our results thus highlight the utility of channel profile analysis to reconstruct the fluvial response to both active tectonism and external changes in base level.

Citation: Harkins, N., E. Kirby, A. Heimsath, R. Robinson, and U. Reiser (2007), Transient fluvial incision in the headwaters of the Yellow River, northeastern Tibet, China, *J. Geophys. Res.*, *112*, F03S04, doi:10.1029/2006JF000570.

1. Introduction

[2] Recognition of feedbacks among climate, surface processes and tectonics [e.g., *Beaumont et al.*, 1992; *Koons*, 1989] has motivated intensive investigation into the response of landscape form to external forcing. Most of these studies have focused on steady state formulations of fluvial incision rules and their implications for equilibrium river profiles [*Hack*, 1957; *Howard*, 1994; *Mackin*, 1948; *Whipple*, 2004; *Whipple and Tucker*, 1999]. Although application of these rules has met with varying degrees of success in landscapes where a balance between erosion and rock uplift appears to have been achieved [*Kirby and Whipple*, 2001; *Lague and Davy*, 2003; *Snyder et al.*, 2000], such landscapes appear to be the exception, rather than the rule. Many landscapes are argued to be in a transient state, adjusting to changes in tectonic forcing [cf. *Safran et al.*, 2005; *Stock et al.*, 2005], drainage reorganization [*Clark et al.*, 2004], base-level fall [*Anderson et al.*, 2006; *Berlin and Anderson*, 2007], or climate change [*Zhang et al.*, 2001]. Moreover, the form of equilibrium river profiles may be nondiagnostic of the dominant incision process [*Howard et al.*, 1994; *Whipple et al.*, 2000; *Whipple and Tucker*, 2002], whereas the transient response of channel systems to changes in boundary conditions offers an opportunity to refine and test incision rules [*Howard and Kerby*, 1983; *Rosenbloom and Anderson*, 1994; *Whipple*, 2004]. Relatively few tests of this kind have been performed, however [*Bishop et al.*, 2005; *Loget et al.*, 2006; *van der Beek and Bishop*, 2003], largely reflecting the difficulty in characterizing initial conditions, the timing and magnitude of perturbations, and the rates and patterns of channel response. Continued progress in our understanding of the linkages between climate, erosion and tectonics requires additional field sites where the transient response of fluvial systems to a known external forcing can be quantitatively evaluated.

[3] In this paper, we examine the rates and patterns of fluvial incision across the Anyemaqen Shan, a broad mountainous region within the northeastern Tibetan Plateau (Figure 1). Topography in this region is somewhat anomalous

[1]Department of Geosciences, Pennsylvania State University, University Park, Pennsylvania, USA.
[2]Department of Earth Sciences, Dartmouth College, Hanover, New Hampshire, USA.
[3]School of Geography and Geosciences, University of St. Andrews, St. Andrews, UK.
[4]School of Earth Sciences, Victoria University of Wellington, Wellington, New Zealand.

0148-0227/07/2006JF000570

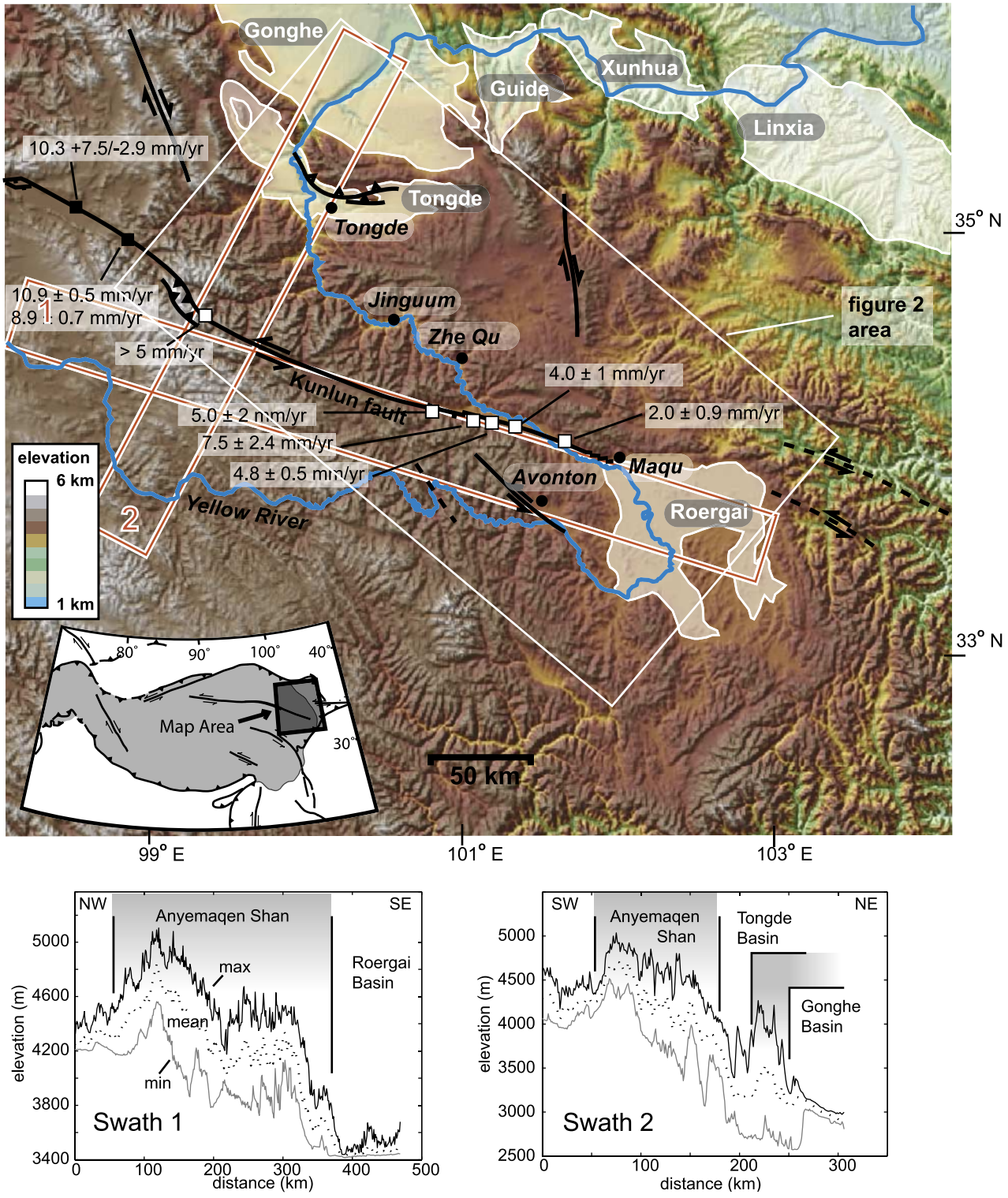

Figure 1. Shaded relief map and topographic swath profiles of a portion of the northeastern Tibetan Plateau. Inset map displays shaded relief map extent relative to the rest of the plateau; areas above 3 km elevation are shaded. The larger map displays the Yellow River (blue line), the approximate boundary between the Yellow River and Yangze watersheds (white line), and identified major active structures (black). The names of terrestrial sedimentary basins along the rivers course are displayed with white text, and locations are outlined in white; the names of several large towns along the Yellow River are displayed in italics. The 30 km wide swath profile extents are delineated by red and white boxes; numbers are keyed to the plots below. On the swath plots, the maximum, mean, and minimum elevations over the 30 km swath window (oriented perpendicular to swath transect) are displayed along with the extents of major topographic features.

relative to the surrounding plateau and is characterized by high relief (>2 km) associated with a deep gorge along the Yellow River. One of the major Eurasian strike-slip faults, the Kunlun fault, transects the range [*Van der Woerd et al.*, 2000], and recent studies of slip along the fault suggest that the fault terminates near the eastern margin of high topography associated with the Anyemaqen Shan [*Kirby et al.*, 2007]. Thus one hypothesis for the association between topography in the range and incision along the Yellow River holds that both are a consequence of differential rock uplift associated with deformation surrounding the tip of the Kunlun fault. However, geologic evidence from exhumed Tertiary-Quaternary basins suggests that recent incision has occurred along the entire course of the Yellow River downstream of the range [*Li et al.*, 1997; *Metivier et al.*, 1998]. The rates and timing of fluvial incision in the Anyemaqen Shan are not well known, but may represent the upstream extent of a transient wave of incision that initiated near the topographic margin of the plateau.

[4] In this study, we evaluate these two hypotheses via a combination of analysis of fluvial channel profiles, determination of fluvial incision rates from dated strath terraces, and estimates of basin-wide erosion rates from cosmogenic isotope concentrations in modern sediment. We begin with a review of geologic observations from sedimentary basins both upstream and downstream of the Anyemaqen Shan that place constraints on the extent of fluvial incision above and below the range. We then explore the distribution of channel gradients throughout the range; this analysis builds on recent work characterizing both equilibrium relations between channel profile steepness and erosion rate [e.g., *Wobus et al.*, 2006c] and the response of channel networks to transient changes in base level [*Crosby and Whipple*, 2006] and tectonic forcing [*Wobus et al.*, 2006a]. Field observations along selected channels complement the topographic analyses and provide quantitative constraints on incision rates. Our results reveal a transient wave of incision, characterized by steep channel gradients and high incision rates (>1 mm/yr) that is associated with basin excavation downstream of the range. Transient fluvial incision, however, is superimposed atop a channel network that exhibits systematic spatial variations in channel steepness and incision rate that we attribute to reflect differential rock uplift across the range. Finally, comparison of the degree of knickpoint propagation, incision rates, and the form of channel profiles to the results of simple models of channel evolution lends insight into the transient behavior of this fluvial network.

2. Fluvial Incision Along the Yellow River

2.1. Topography and Geology in the Anyemaqen Shan

[5] The Anyemaqen Shan is a broad, elliptical region of moderately high elevation and high relief that stands above the Tibetan Plateau between longitudes ~99°E and ~102°E (Figure 1). The range marks a pronounced step from the Tibetan Plateau to the south and west with mean elevations ~4500 m to somewhat lower-elevation regions of the plateau (~3500 m) to the north and east (Figure 1, inset). In contrast to the subdued relief of the plateau, mean elevations within the range exceed 5000 m and local relief approaches 2 km.

[6] The origin of the high topography in the Anyemaqen Shan is somewhat enigmatic. The range is underlain by fine-grained, low-grade metasedimentary rocks of the Songpan Garze complex, an extensive terrane of turbiditic flysch that accumulated during the Middle and Late Triassic [*Bruguier et al.*, 1997; *Weislogel et al.*, 2006; *Zhou and Graham*, 1996] (Figure 2). Although local variations in lithology (primarily Paleozoic limestone and Mesozoic plutons [*Zhengqian et al.*, 1991]) appear to be more resistant to erosion and locally hold up high peaks, there is no significant lithologic difference between bedrock within the Anyemaqen Shan and regions of the plateau that surround it. Thus bedrock susceptibility to erosion and weathering does not appear to be an adequate explanation for the higher relief in the range relative to the surrounding plateau.

[7] The range is bisected from west to east by the Kunlun fault, a active left-lateral strike-slip fault [e.g., *Van der Woerd et al.*, 2000] (Figure 1). A restraining bend in the fault appears to be responsible for the highest peaks within the range, the Anyemaqen massif (~6280 m). This narrow massif is restricted to the fault zone, however, and the relationship of the broader region of high topography to the fault is uncertain. *Kirby et al.* [2007] present evidence that active displacement on the Kunlun fault dies out near the eastern end of the range, implying that displacement must somehow be absorbed by deformation of the crust surrounding the fault tip. One goal of our study is to determine whether incision of the Yellow River and its tributaries across the range may be a consequence of active differential rock uplift between the range and the surrounding plateau.

2.2. Character of the Yellow River Through the Anyemaqen Shan

[8] The Yellow River heads on the plateau to the north and west of the Anyemaqen Shan, transects the range south of the Kunlun fault, makes a broad turn around the eastern end of the fault, and transects the range again on its northern side (Figures 1 and 2). Where the river crosses the range south of the Kunlun fault, it is inset into a series of incised meanders and deep canyons. The river and its tributaries occupy steep walled valleys with few preserved terraces, and intermittently expose bedrock on the channel bed. However, in the Roergai (Zoige) basin, east of the range, the river is a low-gradient, highly sinuous alluvial (sand-bedded) channel. Reconnaissance observations suggest that the river is actively aggrading. Numerous tributaries of the Yellow River do not drain into the trunk stream but are rather ponded behind levees of the trunk channel; during the wet season these valleys form shallow lakes and swamps. As the river exits the northwest corner of the basin and again approaches the higher topography of the Anyemaqen Shan, it transitions from depositional to actively incising. Flights of Holocene fluvial terraces preserved along the river change downstream from fill terraces to bedrock straths [*Kirby et al.*, 2007]. These terraces progressively diverge from the profile of the river, and in the center of the Anyemaqen (near Jinguum, Figure 2), flights of extraordinarily well-preserved strath terraces range up to ~300 m above the river and are capped by ~5–10 m of fluvial gravels and highly variable thickness of loess. Bedrock is frequently exposed along the channel bed in this reach of

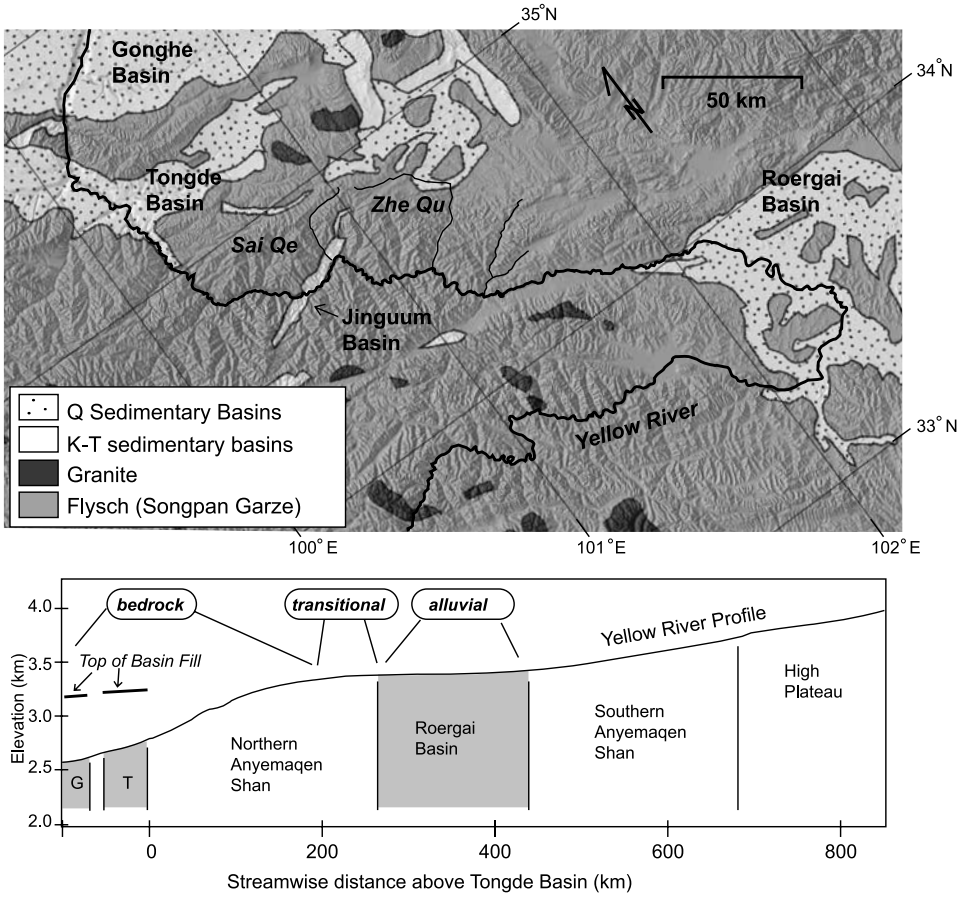

Figure 2. Simplified geologic map of the Yellow River watershed between the Roergai and Gonghe basins (area extent delineated in Figure 1) and channel long profile from the same extent. Major terrestrial sedimentary basins are labeled. Large tributaries to the Yellow River discussed in the text are named in italics. Observations of river incisional character are shown by white dotted areas and are keyed to the profile below. On the long profile, the elevations of the tops of the Gonghe and Tongde (shaded regions labeled G and T) are shown.

the river, and channel gradients steepen downstream throughout the northern part of the range forming a broadly convex longitudinal profile (Figure 2). Tributaries to the Yellow River in the northern Anyemaqen Shan exhibit similar profiles, with relatively low-gradient headwater reaches that become dramatically steeper and more incised approaching their junction with the Yellow River (Figure 3). The morphology of the Zhe Qu displayed in Figure 3 is typical of tributaries in the northern Anyemaqen Shan, with channels that transition from gravel bedded channels with wide floodplains to steep bedrock rivers inset in narrow gorges. The tops of the gorges are marked by broad strath surfaces with gravel treads that are continuous with floodplains upstream of the gorges. These observations qualitatively suggest that the Yellow River has experienced a pulse of recent incision in the northern Anyemaqen, to which the landscape has not yet fully responded.

2.3. Recent Terrestrial Basin Formation and Exhumation

[9] The history of sediment accumulation and excavation in basins immediately upstream (Roergai) and downstream (Tongde) of the Anyemaqen Shan provide additional observations that bear on the evolution of the Yellow River and its tributaries along this reach. Sediment accumulation in the Roergai basin appears to be spatially variable, but a core retrieved from near the Yellow River records >300 m of lacustrine and fluvial silt that accumulated in the past ~1 Ma [*Wang and Xue*, 1996], suggesting that aggradation has been relatively long lived in the basin. Moreover, the absence of thick sedimentary fills within the Anyemaqen Shan coupled with deposition in the Roergai basin might reflect differential rock uplift between the range and the plateau, as the Yellow River attempts to maintain its course over an actively uplifting bedrock sill by aggrading upstream of the sill and incising downstream [e.g., *Humphrey and Heller*, 1995].

[10] In contrast, downstream of the range, the Yellow River passes through two large Tertiary-Quaternary basins, the Gonghe and Tongde basins (Figures 1 and 2), separated from one another by a bedrock range (He Ke Nan Shan). Basin fill consists of primarily undeformed, unconsolidated to poorly lithified fluvial sand and gravel. The tops of sedimentary fill in these basins are extensive low-relief surfaces that gently grade toward the present-day position of the Yellow River, and facies variations suggest that basin filling was driven largely by aggradation along the river and tributaries. In both basins, however, the Yellow River has

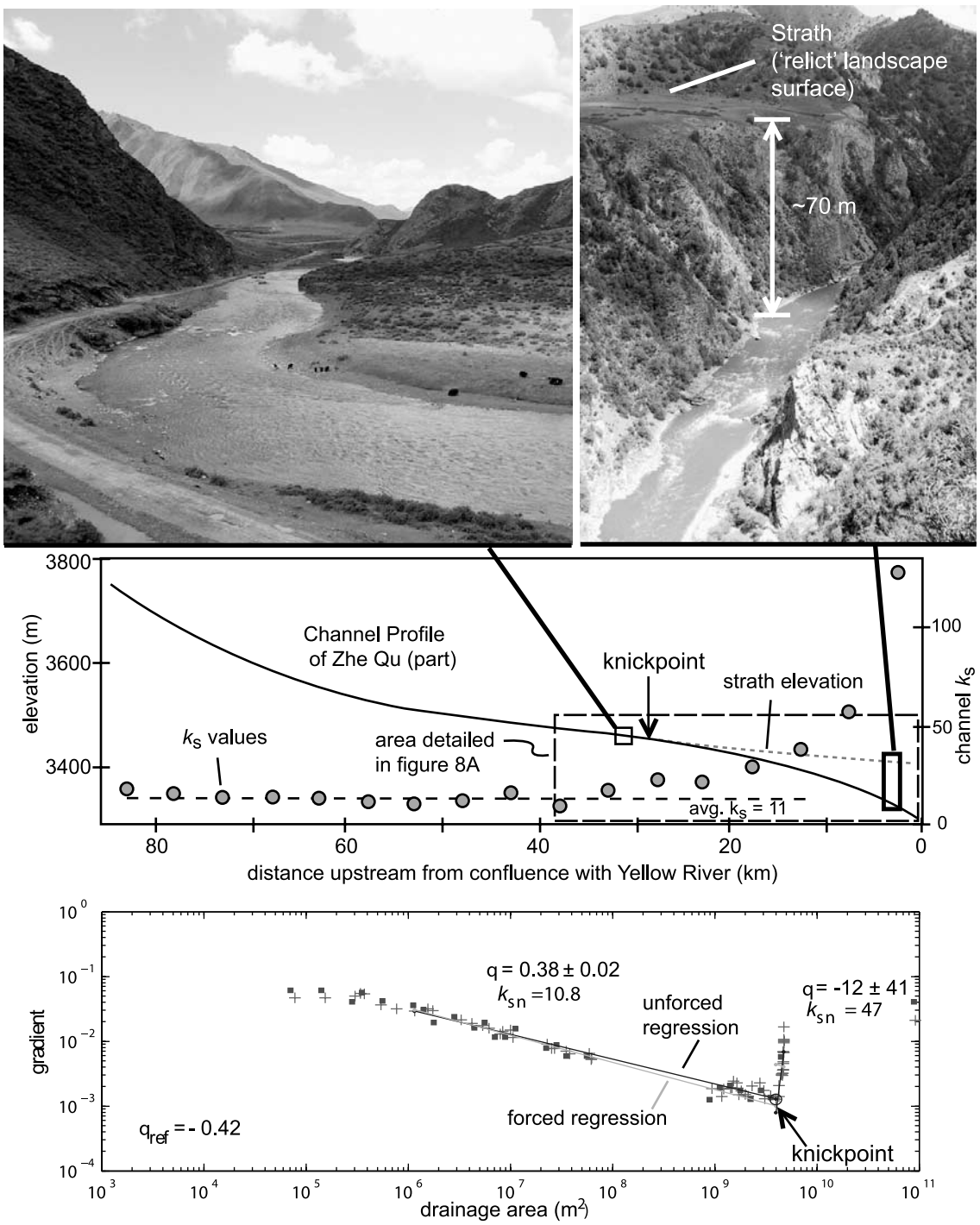

Figure 3. Photographs and channel topographic data from Zhe Qu. Photographs are keyed to (top plot) channel locations identified on the long profile. Channel k_s values, calculated over 5 km sample windows, are displayed as solid circles, and the elevation of the uppermost strath is given by the dashed line. (bottom plot) Gradient versus area plot for the entire channel extent. Both unforced and forced (using a reference θ of 0.42) slope regressions are displayed for channel extents both above and below the identified knickpoint. Raw θ values for each regressed extent are shown along with the forced regression channel steepness (k_{sn}).

incised a deep gorge 400–500 m into the basin fill [*Metivier et al.*, 1998]. This incision has been recorded by a well-preserved flight of terrace surfaces along both sides of the river.

[11] Although detailed chronology of the Tongde and Gonghe basin fill is uncertain, fossils recovered from the lower portions of the exposed section in Tongde suggest Late Pliocene–Early Pleistocene ages [*Zhengqian et al.*, 1991]. Abandonment of the basin fill appears to record a

significant shift from deposition to incision that must have occurred during the Middle or Late Pleistocene. A similar change from deposition to incision is recorded in Late Tertiary basins further downstream along the Yellow River at ca. 1.7 Ma [*Li et al.*, 1997]. Although the mechanism responsible for driving incision remains uncertain, it appears that fluvial excavation of these basins is a response to progressive headward erosion along the Yellow River. Regardless of ultimate cause, the excavation of >500 m of sediment from the Tongde basin represents a direct change in local base level for the Yellow River upstream [e.g., *Anderson et al.*, 2006]. The second goal of our study is to characterize the extent to which the Yellow River and its tributaries have responded to this relative drop in base level.

3. Approach and Background

[12] We seek to deconvolve the influence of differential rock uplift across the Anyemaqen Shan from transient incision driven by downstream changes in local base level during excavation of the Tongde Basin. Our approach is twofold; first, we examine the topographic characteristics of fluvial networks throughout the Anyemaqen Shan. We focus specifically on the identification and characterization of downstream increases in channel gradient (herein referred to as "knickpoints") and their distribution throughout the network. We also characterize channel profile steepness (a measure of channel gradient normalized for differences in contributing drainage basin area, see below) upstream and downstream of knickpoints. Second, we utilize measurements of the timing and rate of fluvial incision reconstructed from terrace sequences in conjunction with cosmogenic isotope inventories in modern sediment to reconstruct the pace of transient landscape evolution.

3.1. Topographic Scaling in Fluvial Systems

[13] Longitudinal profiles of channels in widely varied tectonic and climatic settings typically exhibit a power law scaling between local channel gradient (S) and contributing drainage area (A) [e.g., *Flint*, 1974; *Hack*, 1973; *Howard and Kerby*, 1983],

$$S = k_s A^{-\theta} \tag{1}$$

where k_s is the channel steepness index (a measure of channel gradient normalized for contributing drainage area), and θ is the concavity index (a measure of the rate of change of channel gradient with drainage area). Empirical studies suggest that the concavity index θ commonly falls in a restricted range of values between 0.3 and 0.6 and appears to be independent of rock uplift/erosion rate [*Kirby and Whipple*, 2001; *Tucker and Whipple*, 2002; *Whipple and Meade*, 2004; *Wobus et al.*, 2006a]. Moreover, numerous simple models for fluvial incision into bedrock predict power law relations between channel gradient and drainage area of the form of equation (1) [*Howard et al.*, 1994; *Whipple*, 2001; *Whipple and Tucker*, 1999; *Willgoose et al.*, 1991]. At steady state, the steepness index, k_s, is expected to depend on rock uplift rate [*Lague and Davy*, 2003; *Snyder et al.*, 2003; *Wobus et al.*, 2006a], but the functional relationship between channel steepness and rock uplift may be influenced by a range of factors including, substrate erodibility, channel hydraulic geometry [*Duvall et al.*, 2004; *Finnegan et al.*, 2005], thresholds for erosion [*Snyder et al.*, 2003], a potential role for debris flows [*Stock and Dietrich*, 2003], and thresholds in sediment flux and transport stage [*Sklar and Dietrich*, 1998, 2001, 2004]. It is important to note that the scaling expressed in equation (1) strictly describes the fluvial portion of the channel system. As a result, this relationship holds only above a certain critical drainage area [*Montgomery and Foufoula-Georgiou*, 1993; *Stock and Dietrich*, 2003; *Tarboton et al.*, 1989].

[14] As has been often noted [e.g., *Howard et al.*, 1994; *Stock and Montgomery*, 1999; *Whipple*, 2004], simple models of fluvial incision that assume that erosion rate scales with local bed shear stress and/or unit stream power allow the steady state channel gradient in equation (1) to be written in terms of the rock uplift rate (U) and drainage area [*Whipple and Tucker*, 1999],

$$S_e = \left(U/K\right)^{1/n} A^{-m/n} \tag{2}$$

where K is a coefficient that describes channel erodibility and m and n represent exponents on the erosion rule (stream power or shear stress, see *Whipple* [2004]).

3.2. Transient Channel Response

[15] Equation (2) predicts that equilibrium channels experiencing spatially uniform rock uplift should exhibit a linear relationship between channel gradient and drainage area on a logarithmic plot (Figure 3). Sharp breaks in this scaling, such as a shift of a linear array to greater or lesser gradient, are expected to occur across spatial gradients in uplift rate [*Kirby and Whipple*, 2001] and at contrasts in rock erodibility [*Moglen and Bras*, 1995]. Breaks in these data may also represent transient adjustment of channel gradients to as a wave of incision sweeps through the channel profile following a change in uplift rate and/or change in base level [*Whipple and Tucker*, 1999, 2002]. In such cases, channel profiles are often characterized by an upstream migrating convexity (herein defined as a knickpoint) that separates channel reaches with different channel steepness [e.g., *Crosby and Whipple*, 2006].

[16] The upstream migration of knickpoints has been suggested as the primary mechanism of landscape adjustment to a change in base level or rock uplift rates [e.g., *Nott et al.*, 1996], and it has been recognized that simple detachment-limited models of fluvial incision predict that knickpoints should migrate as a kinematic wave [e.g., *Rosenbloom and Anderson*, 1994]. In the case of a step function increase in uplift rates or drop in base level, channel response to the increased incision rates associated with these events will be characterized by progressive replacement of the channel profile with gradients adjusted to the new forcing [e.g., *Niemann et al.*, 2001; *Whipple*, 2001]. Provided that profile concavity is independent of the rock uplift rate, knickpoint propagation throughout a fluvial network previously at equilibrium will proceed in rather simple fashion. The horizontal component of the knickpoint velocity will depend on upstream drainage area, with ever decreasing velocity as knickpoints move toward smaller drainage area [*Berlin and Anderson*, 2007; *Crosby and Whipple*, 2006; *Whipple and Tucker*, 1999], but the vertical component will be uniform throughout a watershed

[*Niemann et al.*, 2001]. This behavior makes a readily testable prediction; if knickpoints migrate at uniform rate up the channel network, at any point in time they should be at the same elevation [*Wobus et al.*, 2006a]. Note that this result makes no assumption regarding the form of the erosion law, but rather follows from geometric constraints [*Niemann et al.*, 2001; *Wobus et al.*, 2006a].

[17] By way of comparison, models of fluvial incision that explicitly consider the role of sediment flux, either purely transport-limited models [e.g., *Whipple and Tucker*, 2002; *Willgoose et al.*, 1991], or those that incorporate a dual role for sediment in both channel bed erosion and armoring [e.g., *Sklar and Dietrich*, 2004] suggest that the transient fluvial response may be more complex. The response of hillslope and sediment delivery to a change in incision rate along the channel may drive a diffusive adjustment in channel gradient [e.g., *Sklar and Dietrich*, 1998, 2001; *Tucker and Slingerland*, 1997; *Whipple and Tucker*, 2002]. Under certain conditions, thresholds in transport state and/or sediment flux may lead to knickpoint stagnation at threshold drainage areas [e.g., *Crosby and Whipple*, 2006], or even generate "hanging" fluvial valleys as a consequence of the inability of tributaries to maintain pace with trunk streams [*Wobus et al.*, 2006a]. In addition, the response of channel gradients downstream of knickpoints may exhibit nonlinear responses characterized by initial "overshooting" of equilibrium gradients [*Gasparini et al.*, 2006]. In principle, at least, the first means of discriminating between such models is to examine the response of a wide range of tributaries across a watershed experiencing a transient increase in incision rate [*Berlin and Anderson*, 2007; *Bishop et al.*, 2005; *Crosby and Whipple*, 2006].

4. Methods

4.1. Channel Profile Analysis

[18] To test competing hypotheses for apparent differences in incision along the Yellow River, we examined topographic characteristics of tributary channel profiles between the Roergai and Tongde basins (Figure 1). Channel profiles of 168 tributaries to the Yellow River in the Anyemaqen Shan were extracted from digital topographic data from the SRTM (Shuttle Radar Topography Mission) archive. The relatively coarse resolution of the DEM (3 arc sec) restricted our analysis to watersheds greater than 1 km^2 in total area. Channel profiles were extracted and analyzed following *Snyder et al.* [2000] and *Kirby et al.* [2003]. We removed spikes along the channel profile and smoothed the data using a moving average of 20 pixels. This window size was determined to adequately maintain the overall form of the channel profile, while removing high-frequency noise associated with the topographic data. Channel gradients were determined over a fixed vertical interval of 10 m [cf. *Wobus et al.*, 2006c].

[19] Regression of linear arrays of channel gradient versus drainage area yielded estimates of steepness and concavity indices for each of the tributary profiles (e.g., Figure 3, bottom plot). The upstream limit of regressions was chosen by visual inspection of a break in scaling between channel gradient and drainage area. This point is interpreted to represent the transition from hillslope and/or colluvial channels to the fluvial portion of the network and was generally found to occur at a contributing drainage area of $\sim 10^6$ m^2. In addition, regression of the same data was conducted with a fixed, reference concavity to yield estimates of a normalized steepness index (k_{sn}). This value is observed to scale with erosion rate in a variety of tectonic settings [e.g., *Kirby and Whipple*, 2001; *Lague and Davy*, 2003; *Safran et al.*, 2005; *Wobus et al.*, 2006c]. We chose a value of 0.42 for the reference concavity (θ_{ref}) on the basis of the mean concavity of channel profiles above knickpoints (see supplemental data[1]). Uncertainties in k_{sn} values are determined from the regression parameters (see Appendix A for a discussion of uncertainty analysis).

[20] If tributary channels exhibited smooth profiles, regressions were truncated at the tributary junction with the Yellow River, and channels are well characterized by a single value of k_{sn}. However, where channels exhibited downstream increases in gradient associated with convex knickpoints (see example in Figure 3), channel reaches above and below knickpoints were regressed separately. Knickpoints were identified by a step in linear arrays of gradient drainage area data toward higher gradients (Figure 3). In many tributaries, downstream increases in channel occur over several kilometers of channel length and are associated with a progressive downstream increase in k_{sn} values (Figure 3). As a consequence, we identified the top of the zone of increased gradient as the position of the knickpoint. This definition was chosen to provide a consistent measure of the upstream extent of influence of recent fluvial incision.

[21] Processing of channel topographic data imparts a degree of uncertainty to determination of the position of knickpoints in the landscape. We take the width of the smoothing window as a conservative estimate of uncertainty on the horizontal position along the channel profile, reasoning that the knickpoint must be located within this distance of its actual location on the profile. Uncertainties on the elevation of knickpoints were calculated as the product of channel slope tangent to the identified point and the probability distribution of point horizontal locations based on the smoothing window size.

4.2. Measures of Erosion Rate

[22] In order to relate differences in channel profile form to erosion rate, we utilize two measures of erosion rates in the landscape. Abandoned fluvial strath terraces provide a measure of average incision rates in the fluvial network downstream of knickpoints. Terrace surfaces above the Yellow River and tributaries were surveyed with a laser rangefinder. Samples of fluvial sediment from terrace treads place bounds on the timing of fluvial occupation of the surface. All samples in this study were dated by either ^{14}C of detrital organic material (charcoal or snail shells) or optically stimulated luminescence (OSL) of floodplain silt. Neither method directly dates abandonment of the terrace, and therefore our incision rates are minimum estimates. Locations of terrace surveys are shown on Figure 4. Details of the OSL determinations are provided in the supplementary material.

[23] To complement fluvial terrace records of incision rate, we analyzed the concentration of ^{10}Be in modern

[1] Auxiliary material data sets are available at ftp://ftp.agu.org/apend/jf/2006jf000570. Other auxiliary material files are in the HTML.

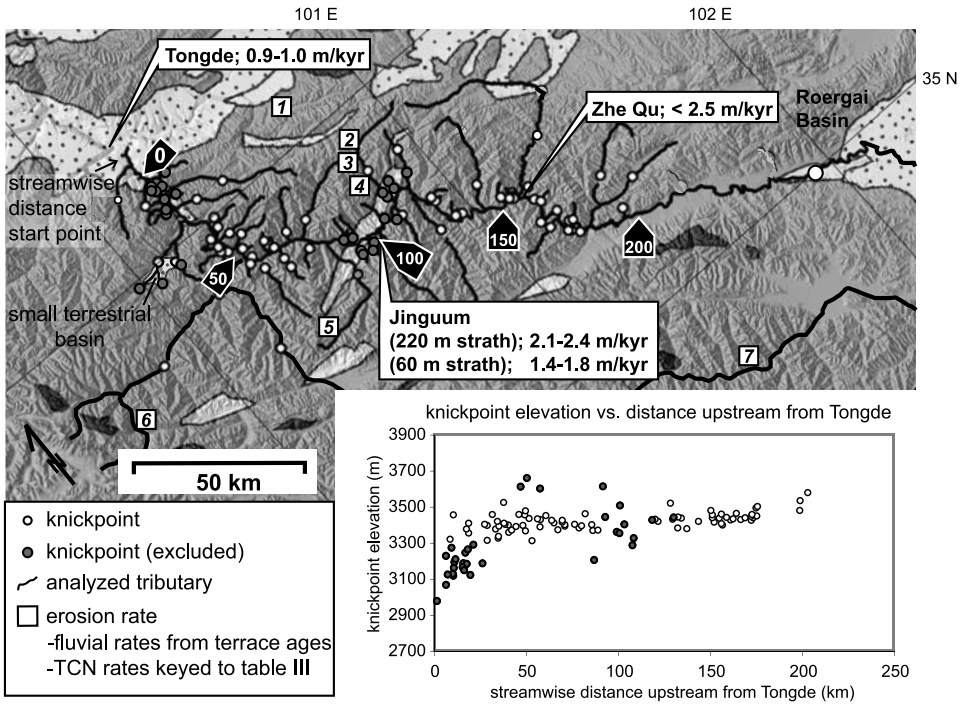

Figure 4. Simplified geologic map of the Yellow River watershed between the Roergai and Gonghe basins and plot of all identified knickpoint elevations. On the map, analyzed tributary extents are delineated along with the locations of knickpoints. River incision rate estimates (in mm/yr) from terrace ages are displayed, and catchment erosion rates from sediment ^{10}Be determined exhumation rate sample locations are keyed to Table 3. Streamwise distance kilometer markers along the yellow river upstream of Tongde are shown by the black boxes with white lettering. On the plot, knickpoint elevations are plotted against point streamwise distance upstream of Tongde. The starting point for the streamwise distance measure used on all plots in this work is shown. Solid knickpoint symbols on both the map and the plot represent points excluded from this analysis because of their association with basin sediment/bedrock contacts.

sediment from second- and third-order catchments throughout the study area. Provided that stream sediment is well mixed and that target minerals are equally distributed throughout a watershed, the concentration of cosmogenic ^{10}Be in modern stream sediment can provide an estimate of the spatially averaged erosion rate in the watershed [e.g., *Balco and Stone*, 2005; *Brown et al.*, 1996; *Gosse and Phillips*, 2001; *Granger et al.*, 1996; *Lal*, 1991]. Such methods have been recently shown to provide an important guide to the distribution of erosion rate across tectonically active landscapes [*Wobus et al.*, 2005].

[24] Sediment samples composed of course sand and gravel were extracted from active channel beds of 7 tributaries to the Yellow River. Samples were extracted exclusively from fine gravel bars that were partially or fully submerged in the active channel. Tributary catchments with obvious evidence of landslides or large amounts of headwater sediment storage were avoided. All samples were collected at or above knickpoints and thus provide a measure of erosion rates in the "relict" portion of the landscape. To avoid contamination by sediment stored in terraces, all samples were collected upstream of channel reaches that cut across alluvial fan or terrace surfaces. We extracted pure quartz from sediment samples by physical and chemical separation at the Terrestrial Cosmogenic Nuclide Lab at Dartmouth College. Beryllium was isolated via acid digestion of quartz and anion column chemistry. After precipitation as beryllium oxide, sample material was packed onto targets and sent for isotopic concentration measurement at the accelerator mass spectrometry facility at Purdue University (PRIME lab).

[25] We account for topographic shielding, elevation, and latitude variation in ^{10}Be production in quartz within sampled basins were determined using SRTM DEM data. This topographic data was processed using MATLAB and ARCGIS codes to determine an adjusted ^{10}Be production rate of *Lal* [1991] for each grid cell based on the *Stone* [2000] model of elevation and latitudinal variations in cosmogenic radiation influx. The resultant, combined ^{10}Be production rates for each DEM grid cell within a sampled catchment are then spatially averaged to provide a bulk catchment production rate. Reported errors on these samples are strictly those associated with the AMS analysis of ^{10}Be content and ICP-MS measurement of stable Be content.

5. Results

5.1. Channel Profiles

[26] Analysis of ~300 tributary channel profiles throughout the Anyemaqen Shan reveal a first-order difference above and below the Roergai basin (Figure 4). Tributaries entering the Yellow River above the basin exhibit smooth,

concave-up profiles with no obvious knickpoints along their reaches. Downstream of the basin, however, nearly all tributaries join the Yellow River through oversteepened reaches. This dichotomy is central to our goal of deconvolving transient incision across the range and guides the discussion of our results. We first consider the distribution of knickpoints within the watershed, and then turn to patterns of channel steepness (k_{sn}).

5.1.1. Knickpoint Form and Distribution

[27] Downstream of the Roergai basin we analyzed 116 tributaries to the Yellow River, all of which exhibited a knickpoint near or above their junction with the Yellow River (Figure 4). Comparison of knickpoint locations with bedrock geology revealed that 34 of these knickpoints are coincident with lithologic boundaries (primarily contacts between Tertiary basin fill and the Triassic flysch); these knickpoints are excluded from further analysis. The remaining 82 knickpoints are developed along channels within uniform lithology and exhibiting a single downstream increase in k_{sn}.

[28] Nearly all of the channel profiles downstream of knickpoints exhibit a progressive increase in channel gradient that corresponds to a broad convex channel reach. In many of the larger tributaries, this reach is many times longer than the smoothing window size, indicating that this observed morphology is not simply an artifact of the smoothing we impose on channel profile data. The morphology of the Zhe Qu is typical of observed channel and knickpoint form (Figure 3). Importantly, increases in channel gradient extend the entire distance to the Yellow River; we do not observe the development of a concave downstream reach as would be expected from simple models of knickpoint retreat [e.g., *Gardner*, 1983; *Gilbert*, 1896; *Holland and Pickup*, 1976; *Miller*, 1991; *Nott et al.*, 1996; *Rosenbloom and Anderson*, 1994].

[29] The upstream extent of tributary steepening is confined to a relatively narrow elevation band throughout the northern Anyemaqen (Figure 4, inset). Knickpoints are found between 3200 and 3600 m elevation, but the majority (>70%) occur within a narrow range of elevations between 3350 to 3550 m (mean of 3430 m) (Figures 5a and 6). In order to evaluate whether elevations systematically increase upstream, we take a bootstrap approach to incorporating uncertainties in knickpoint elevations. Each knickpoint was assigned an array of 21 elevation values, distributed uniformly over a range of values corresponding to the 90% confidence interval of knickpoint location. Elevations are weighted by a double-tapered, linear probability distribution function, such that each knickpoint elevation is associated with a range of most likely values. The best fit linear regression of knickpoint elevation versus distance to the entire suite of data indicates that knickpoints occur at slightly higher elevations upstream (Figure 6). Confidence intervals on the slope of the regression, however, reveal that the slope of the regression is not statistically significant at the 95% confidence level (slope of 0.0005 ± 0.0005). Thus, although it appears likely that knickpoints farther upstream from the Tongde basin have migrated higher into the landscape, the uncertainties on knickpoint elevations also allow the possibility that knickpoints sit at a uniform elevation.

[30] Knickpoint elevation also appears to be independent of the drainage area upstream of knickpoints (Figure 5b). Likewise, the difference in elevation between a given knickpoint and the elevation at the tributary junctions with the Yellow River does not depend on upstream drainage area (Figure 5d). The elevation difference, however, decreases with distance upstream of the Tongde basin (Figure 5c), consistent with the observed increase in channel gradient along the Yellow river and its tributaries. Thus the vertical distribution of knickpoints in the landscape is, to first order, uniform and not strongly dependent on watershed topology.

[31] The horizontal positions of knickpoints in the landscape appear to depend on watershed size. Knickpoints show a power law relationship between upstream drainage area and streamwise distance, which reflects the fact that host channels follow Hack's law [*Hack*, 1957] and confirms that knickpoints are positioned within fluvial channels (Figure 5e). Importantly, the horizontal positions of knickpoints are distributed throughout the Yellow River watershed, and do not appear to have stalled at small drainage areas [e.g., *Crosby and Whipple*, 2006]. This suggests that current distribution reflects, to some degree, the rate of migration. The distances of knickpoints upstream of the Yellow River exhibits a power law dependence on contributing drainage area (Figure 5f), consistent with models of knickpoint retreat as a kinematic wave [*Rosenbloom and Anderson*, 1994]. The exact form of this relationship is complicated by scatter imposed by the fact that incision initiated at each tributary junction at different times as the wave of incision migrated up the Yellow River. Overall, the data are consistent with knickpoints as mobile elements of this landscape with a horizontal celerity that depends on contributing drainage area.

5.1.2. Tributary Channel k_{sn} Patterns

[32] As the knickpoints discussed above are likely to be transient features that separate regions of the fluvial network experiencing different rates of forcing [*Wobus et al.*, 2006c], we characterize channel k_s both above and below knickpoints. As noted above, we observe distinct differences in the presence or absence of knickpoints below and above the Roergai basin, respectively. We discuss each region separately.

[33] Above the Roergai basin, we examined 184 tributaries, none of which exhibits marked deviations from a concave upward facing profile. Steepness indices, however, appear to vary systematically across the range (Figures 7 and 8b). These values vary from ~10 to 20 at the edges of the range and increase to a maximum of ~55 in the central extents of the range. We exempted from this analysis channels that exhibited valley morphologies indicative of occupation and erosion by glaciers (Figure 7).

[34] In the northern Anyemaqen Shan, downstream of the Roergai basin, we examined 82 channels. Steepness indices (k_{sn}) of channel reaches upstream of knickpoints range in value from 10 to 60. Lower values are spatially associated with the flanks of the range, with progressively increasing values near the center (Figures 7 and 8a). Tributary k_{sn} values downstream of knickpoints are significantly higher ($k_{sn} \sim 100-200$) and exhibit a large degree of scatter but appear to show a similar overall pattern to the upstream k_{sn} values. Steepness index values range from ~90 near the Tongde basin, increase to ~190 along the transect, and decrease back down to ~70 near the Roergai basin. Impor-

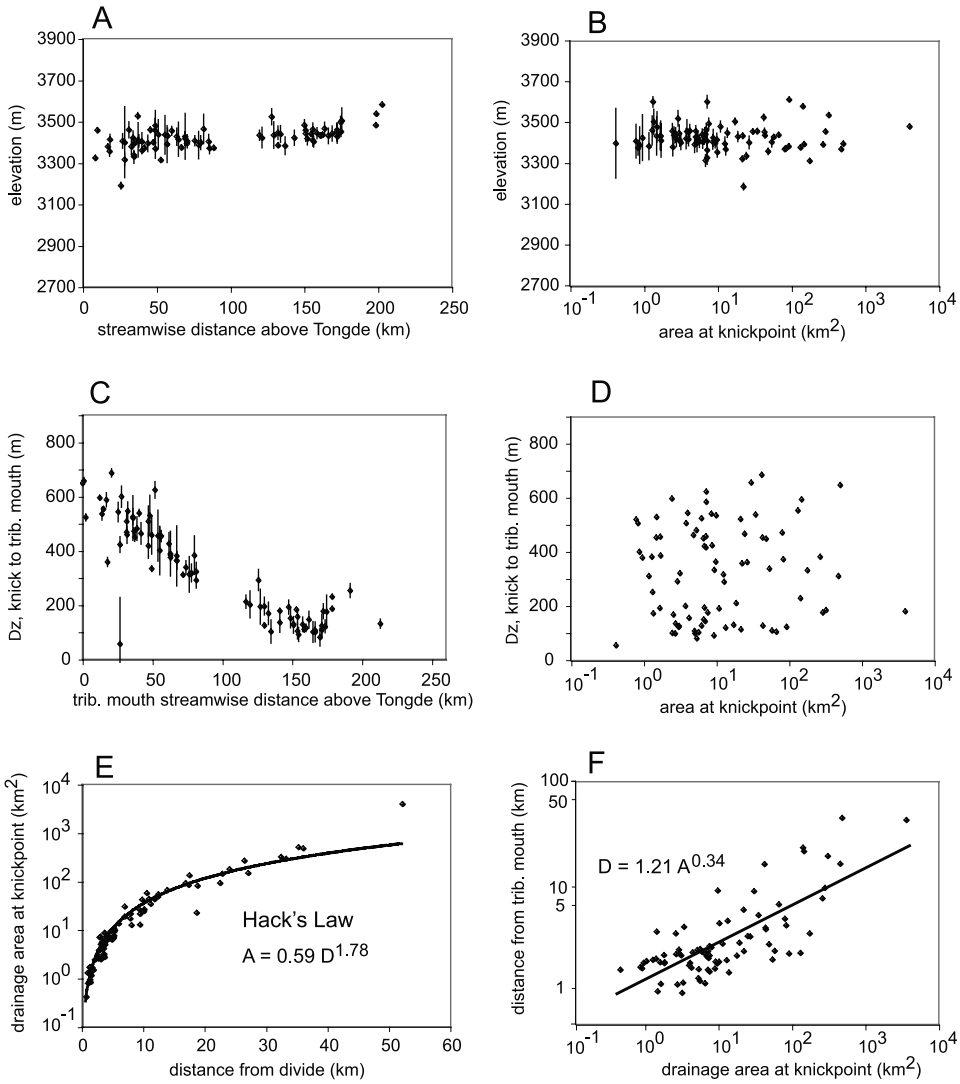

Figure 5. Plots of knickpoint topographic data. Points related to lithologic contacts are excluded. (a) Knickpoint elevation versus streamwise distance above Tongde; 90% confidence interval error bars are shown for knick elevations. See text for error determination. (b) Knickpoint elevation (asl) plotted against catchment area at points. (c) Knickpoint elevation above host tributary mouth elevation plotted against tributary mouth streamwise distance along the Yellow River upstream of Tongde. (d) Knickpoint elevation above host tributary mouth elevation (tributary mouths located at their intersection with the Yellow River) plotted against catchment area upstream of points. (e) Catchment area at knickpoints plotted against point distance from tributary divide. (f) Knickpoint distance from host tributary mouth (intersection with the Yellow River) plotted against catchment area at points.

tantly, k_{sn} values observed above knickpoints in the northern Anyemaqen Shan show a similar distribution of values to those observed along entire tributaries in the southern Anyemaqen Shan, upstream of the Roergai basin. Through both regions, k_{sn} values are low at the edges of the range and increase toward the core of the range.

5.2. Field Determinations of Fluvial Incision and Landscape Erosion

5.2.1. Terrace Ages and Fluvial Incision Rates

[35] Surveyed and dated terrace sequences in the Tongde basin, the Jinguum Basin, and at the outlet of the Zhe Qu provide estimates of incision rate along the steep reach of the Yellow River downstream of the Roergai Basin (Tables 1 and 2 and Figure 4). In the first of these sites, at the southern edge of the Tongde basin, we collected fluvial sand from a strath terrace developed in Quaternary basin fill for OSL dating. Terrace deposits consist of ~10 m of fine to coarse fluvial sand overlying a bedrock strath ~140 ± 1 m above the modern river. Material within the alluvial cap is much finer grained and less consolidated than the underlying cobble to boulder conglomerates of the Tongde basin fill. We interpret the burial age of this sample to record a maximum allowable age for abandonment of the underlying strath; inferred incision rate are thus a minimum. The OSL sample yielded a mean age range of 140.7 ± 8.7 ka (Table 1),

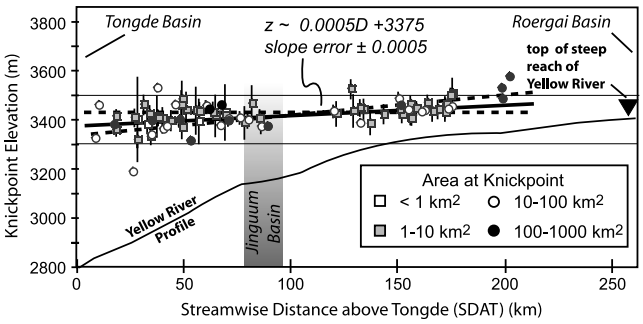

Figure 6. Knickpoint elevations plotted against point streamwise distance upstream of Tongde. Point symbols delineate catchment area at knickpoints, and 90% confidence interval error bars are shown. The modern and reconstructed Yellow River profiles (see section 6 in the text) along this extent are shown along with the location of the Jinguum basin. The trend and equation for a weighted least squares regression through point elevations are shown; minimum and maximum slope error bounds are dashed.

yielding an incision rate between 0.9 to 1.0 m/ka over that time period.

[36] Our second site is located approximately 70 km upstream, near the monastery town of Jinguum (Figure 4). Here, the Yellow River has carved a wide valley into relatively weak Tertiary sediments; flights of strath terraces are present for ~250 m above the river gorge. We obtained samples from three terrace levels that together provide an estimate of how incision rates vary with time. From the highest terrace (240 m above the river), we obtained two OSL samples from a ~10 m thick package overbank silts and fine sands. These two samples yielded overlapping OSL burial ages of 95.6 ± 10.7 ka and 106.1 ± 6.5 ka (Table 1). These data indicate average incision rates since Late Pleistocene of ~2.1–2.8 m/ka since ~100 ka. From the lower terraces, we sampled charcoal and terrestrial shell material for radiocarbon dating. The second terrace (T2) strath sits 60 ± 1 m above the river, and the first terrace (T1) is 6 ± 0.5 m above the river. Terrestrial snail shells were extracted from the upper 2 meters of unconsolidated fluvial gravel capping the T2 bedrock strath surface. Shell material yielded an calibrated ^{14}C age of 38–39 ka (Table 2). Also

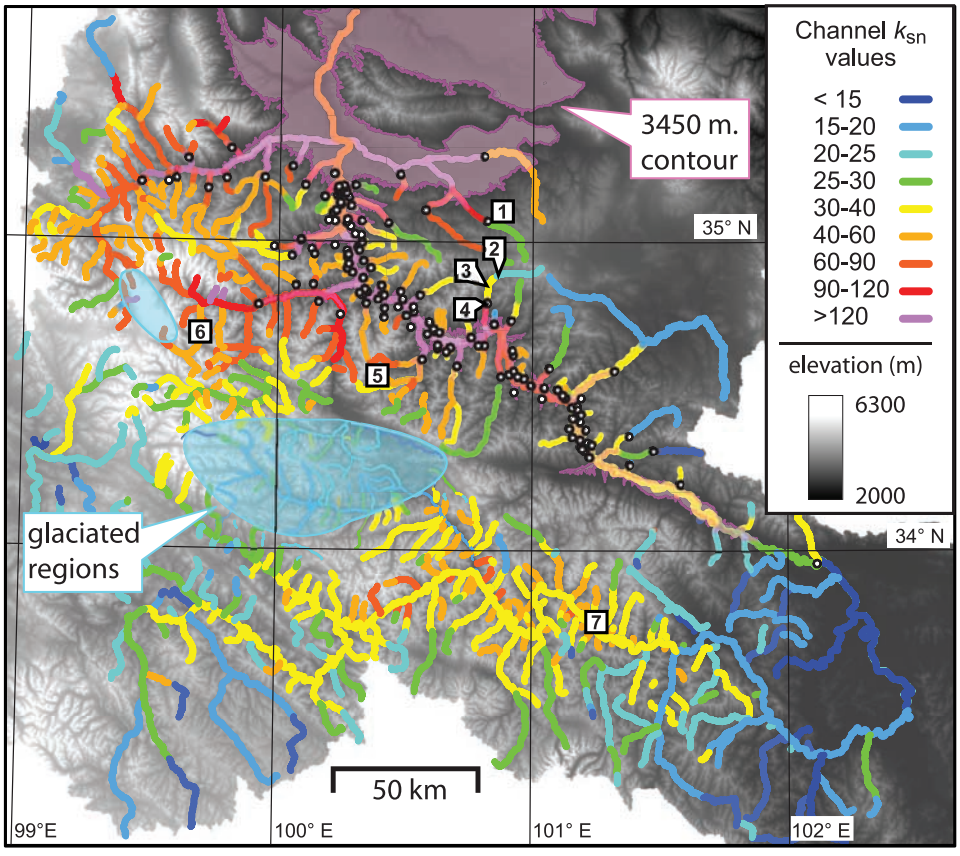

Figure 7. Map of k_{sn} values of all tributaries analyzed and the Yellow River in the Anyemaqen Shan, displayed against a background of elevations within the Yellow River watershed. Approximately 200 tributaries in the northern and southern Anyemaqen were analyzed to produce this figure in addition to those discussed in the text. Knickpoint locations are delineated by the white dots, and areas less than 3450 m elevation are shaded to approximate the limited spatial extent of the incisional wave in the northern Anyemaqen Shan. ^{10}Be determined catchment exhumation rate sample locations are shown in the boxes and are keyed to Table 3. A large region of low k_{sn} values located in the central region of the map is attributed to extensive glaciation at elevations over ~4 km in this area.

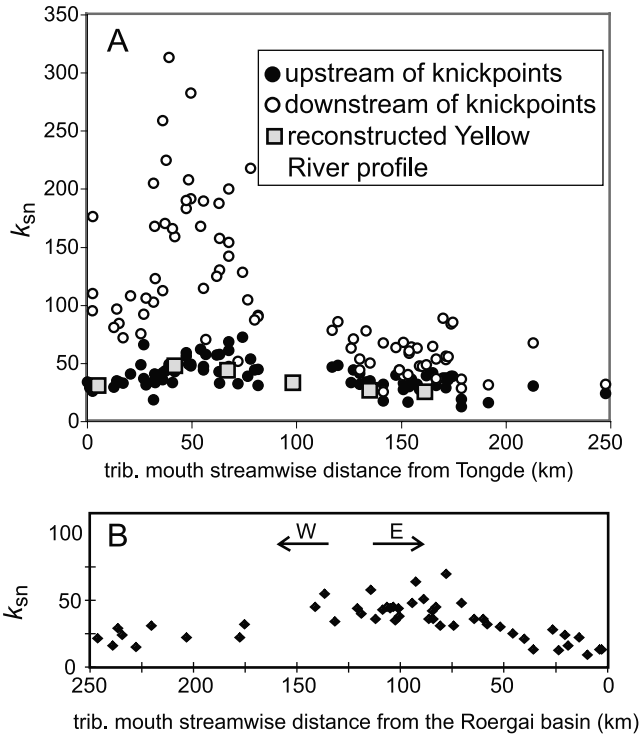

Figure 8. (a) Channel k_{sn} values of tributaries in the northern Anyemaqen Shan, plotted according to their host tributary mouth distance upstream of Tongde. Channel k_{sn} values from both upstream and downstream of identified knickpoints are displayed along with k_{sn} values calculated over ~30 km intervals along the reconstructed, pretransient incision profile of the Yellow River shown in Figure 8e. (b) Channel k_{sn} values of tributaries in the southern Anyemaqen Shan, plotted according to their host tributary mouth distance upstream of the Roergai basin.

from the same terrace tread, an OSL sample extracted from a sand lens within the T2 terrace gravel cap corroborates this range with a burial age of 37.2 ± 2.1 ka (Table 2). Assuming that the river abandoned this surface shortly after sample deposition, incision rates appear to have ranged from 1.5 and 1.7 m/ka. Finally, charcoal extracted near the base of fluvial sand and gravel of the lower (T1) strath yielded a calibrated ^{14}C age of 8.6–9.0 ka BP (Table 2). This represents a minimum incision rate of ~0.7 m/ka.

[37] Our third site is located near the upstream extent of the steep and convex reach of the Yellow River in the northern Anyemaqen Shan. At the junction with the Zhe Qu an extensive strath surface is preserved ~65 m above the river (Figure 4); several lower strath terraces are inset into the steep, bedrock walls that line the Yellow River. The uppermost strath is capped by ~2 m of fluvial gravels, which are in turn overlain by ~2 m of loess. Snail shell fragments extracted from the base of the loess yielded a calibrated ^{14}C age of 30.6–31.3 ka (Table 2). Loess accumulation likely began shortly after abandonment of the terrace tread, although the amount of time elapsed is unknown. As a result, incision rates are somewhat uncertain but appear to exceed ~2.5 m/ka at this site.

[38] Taken together, our results are consistent with the upstream migration of a wave of incision. Although the onset of incision at the downstream extent of our study area, in the Tongde Basin, is somewhat uncertain, extrapolation of the Late Pleistocene rate of ~1 m/yr would yield the observed depth of incision (400–500 m) in 400–500 ka. Altogether we recognize the uncertainty associated with extrapolation of a single age, the broad timing is entirely consistent with the biostratigraphic ages near the base of the section [*Zhengqian et al.*, 1991]. The onset of fluvial incision upstream of the basin appears to be even younger, as suggested by the broad relict floodplains atop the terrace sequence at Jinguum and along the Zhe Qu. In these locations, our chronology suggests that incision did not begin at these locations until subsequent to ~100 ka and ~26 ka, respectively. Moreover, incision rates determined from multiple terrace levels at Jinguum seem to indicate that incision rates have slowed with time (Figure 4), consistent with the passage of an incisional wave generated by base-level fall.

5.2.2. Basin-Wide Exhumation Rates From Sediment ^{10}Be Inventories

[39] Rates of exhumation determined from sediment ^{10}Be inventories extend our estimates of landscape erosion rates above knickpoints [*Granger et al.*, 1996] (Table 3). Seven samples extracted from six different catchments yielded basin-wide erosion rates between ~0.05 and ~0.11 m/ka (Figure 7 and Table 3). These samples were all collected upstream of, or directly adjacent to, the locations of knickpoints in the larger tributaries that join the Yellow River. Sample site 1, located along the approximate northern boundary of the Anyemaqen, yielded the lowest rate of 0.056 ± 0.004 m/ka. Sample sites 2–4 are distributed along a large tributary that joins the Yellow River near Jinguum, the Sai Qe (Figure 7). These samples record increasing erosion rates (from ~0.05 to 0.08 m/ka) in small catchments that intersect the trunk tributary progressively farther downstream and deeper into the Anyemaqen Shan. The sample tributary mouth at site 3 is located ~1 km downstream of the knickpoint identified in Sai Qe. Erosion rates from

Table 1. Optically Stimulated Luminescence Sample Age Control and Context[a]

Location, km Upstream	Sample	U,[b] ppm	Th,[b] ppm	K,[b] %	Cosmic Dose Rate,[c] Gy/ka	Total Dose Rate, mGy/ka	Mean D_e, Gy	Age, ka	Incision Rate, m/ka
Tongde (0)	NHKOSL-2S	1.35 ± 0.014	0.357.04±	1.46 ± 0.07	0.172	2.25 ± 0.11	322.1	140.7 ± 8.7	0.9–1.0
Jinguum (95)	NHKOSL-05-2	3.03 ± 0.18	10.05 ± 0.11	1.81 ± 0.04	0.188	3.99 ± 0.17	148.6	37.2 ± 2.1	1.5–1.7
Jinguum (95)	NHKOSL-05-3	2.79 ± 0.30	11.83 ± 0.15	2.58 ± 0.06	0.119	4.47 ± 0.30	427.2	95.6 ± 10.7	2.2–2.8
Jinguum (95)	NHKOSL-05-4	2.84 ± 0.28	9.68 ± 0.13	1.87 ± 0.04	0.148	3.50 ± 0.17	370.8	106.1 ± 6.5	2.1–2.4

[a]Samples were analyzed at the Victoria University of Wellington except for sample NHKOSL-2S, which was analyzed at the University of St. Andrews.
[b]U, Th, and K were calculated using ICP-MS.
[c]Cosmic dose rate was calculated assuming constant burial depth using method described by *Prescott and Hutton* [1994]. Uncertainty was taken as 10%.

Table 2. ^{14}C Sample Age Control and Context[a]

Location, km Upstream	Sample	Material	Strath Height, m	$d^{13}C$	^{14}C Age, years BP	Age Range, years BP	Rate Range, m/ka
Jinguum (95)	EK-K-3	charcoal	6 ± 1	−23.7	7,945 ± 62	8,610–9,000	0.6–0.7
Jinguum (95)	NH-KC-05-1	snail shells	60 ± 2	−7.0	33,550 ± 550	38,375–39,493[b]	1.5–1.6
Zhe Qu (153)	NH-KC-05-4	shell fragments	65 ± 3	−6.7	25,740 ± 280	30,617–31,279[b]	2.0–2.2
Avonton 1 (540)	NH-KC-05-12	shell fragments	9 ± 1	−6.1	16,580 ± 460	18,610–21,049	<0.5
Avonton 2 (520)	NH-KC-05-13	snail shells	10 ± 1	−6.8	14,538 ± 80	16,955–18,016	<0.64

[a]All younger samples calibrated using Calib 4.3 [*Stuiver et al.*, 1998]. Strath height refers to elevation above modern channel.
[b]Because of advanced sample age, calibration was based on constraints from *Fairbanks et al.* [1990].

samples 4A and 4B may therefore contain some component of transient incision. Site 5, located to the southwest of Jinguum, records an erosion rate similar to site 4 (∼0.08 m/ka). Site 6, located in the highest-relief area of the Anyemaqen Shan, records the highest ^{10}Be determined erosion rate (∼0.11 m/ka). Site 7, which is a catchment that drains directly into the Yellow River upstream of the Roergai basin, records a lower rate of ∼0.07 m/ka. Overall, the results of the ^{10}Be analysis indicate that most parts of the landscape upstream of knickpoints are experiencing relatively slow rates of erosion (<0.11 m/ka).

6. Relict Landscape Reconstruction

[40] The presence of a low-relief landscape, gentle channel gradients and slow erosion rates upstream of knickpoints in the northern Anyemaqen Shan suggests that this landscape is ''relict'' in the sense that topography reflects conditions prior to onset of rapid incision along the Yellow River [e.g., *Crosby and Whipple*, 2006]. In this section we present arguments that channel gradients in this landscape were likely adjusted to spatial variations in erosion rate. Moreover, we utilize both field surveys and DEM-generated channel profiles to reconstruct the relief on the relict channel network and to place bounds on the preincision shape of the Yellow River longitudinal profile.

6.1. Evidence for Adjusted Channel Profiles

[41] A number of topographic characteristics point to the presence of a landscape at or near a steady state in the northern Anyemaqen Shan prior transient fluvial incision along the Yellow River. First, the concavities of channel profiles (θ) above knickpoints and in the southern Anyemaqen Shan (upstream of the Roergai basin) both exhibit mean values ∼0.4–0.45, consistent with theoretical and empirical determinations of profile concavity in regions of steady state [e.g., *Kirby and Whipple*, 2001; *Whipple and Tucker*, 1999; *Wobus et al.*, 2006c]. Although a uniform concavity is not a sufficient condition to prove steady state conditions, as transient profiles of transport-limited channels may remain smooth and free of convexities [*Whipple and Tucker*, 2002], it is consistent with streams in a ''graded'' state. Second, field observations reveal that channels above knickpoints are gravel bedded and reside in broad, alluvium-filled valleys (Figure 3); terraces indicative of recent incision are typically low (<5–10 m) or absent. These observations are again consistent with a landscape in which the channels are transport-limited and simply conveying sediment downstream. Finally, systematic spatial variations in channel steepness (k_{sn}) above knickpoints in the northern Anyemaqen Shan (Figures 7 and 8) are matched by spatial variations in the southern part of the range (upstream of the Roergai basin). This correspondence is striking, and seems to indicate that both sets of tributaries are responding to a spatial forcing, likely variations in rock uplift rate. The fact that the position, wavelength, and magnitude of the variations in k_{sn} are similar argues that channels upstream of knickpoints are adjusted to this forcing.

6.2. Covariation of Incision/Erosion Rate and Channel Steepness

[42] Observations of channel gradients paired with fluvial incision and landscape erosion rates determined in this study provide an opportunity to empirically determine the functional relationship between k_{sn} and incision/erosion rate. Measured river incision and ^{10}Be determined basin erosion rates are compared to the k_{sn} value of adjacent channels (Figure 9). Adjacent channel k_{sn} values were determined as the mean of trunk tributary values and values of smaller catchments within 2–3 km of sample sites. Typically, the variance within each collection of k_{sn} values is low (<10) and supports the use of these mean values to describe channel slopes near each sample site.

[43] Our results reveal a positive relationship between channel steepness (k_{sn}) and catchment erosion rate across the range of our data (Figure 9). Although the data present a

Table 3. Basin-Wide Erosion Rates Determined From Terrestrial Cosmogenic Nuclide Accumulations

Site	Sample ID	Location	Elevation Range, m	Basin Size, km^2	Production Rate, atoms/g quartz/yr	^{10}Be, atoms/g quartz	e(^{10}Be), atoms/g quartz	Erosion Rate, m/ka
1	NH-KE-04-2	N 34.10°, E 100.761°	3500–3700	1.43	57	125,766	2,845	0.056 ± 0.004
2	NH-KE-04-3	N 34.898°, E 100.885°	3590–3850	0.84	67	634,156	3,135	0.059 ± 0.005
3	NH-KE-04-4A	N 34.799°, E 100.811°	3420–3810	0.91	57	707,902	4,107	0.083 ± 0.006
3	NH-KE-04-4B	N 34.797°, E 100.811°	3395–3810	1.03	57	426,520	2,237	0.081 ± 0.006
4	NH-KCB-05-1	N 34.777°, E 100.813°	3580–4010	2.31	58	439,792	13,786	0.084 ± 0.007
5	NH-KCB-05-3	N 34.526°, E 100.394°	3792–4320	5.01	75	545,990	80,426	0.085 ± 0.017
6	NH-KCB-05-2	N 34.752°, E 99.693°	3900–4900	4.12	77	448,257	16,764	0.107 ± 0.009
7	NH-KCB-05-6	N 33.693°, E 101.388°	3520–3610	2.24	64	567,528	21,790	0.070 ± 0.006

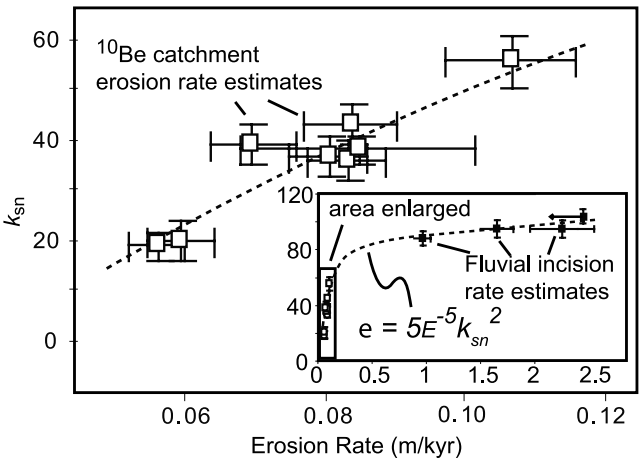

Figure 9. River incision rates measured from strath terrace position (black boxes) and ^{10}Be determined catchment erosion rates (white boxes) plotted against measured k_{sn} values of proximal channels; k_{sn} values were determined as the average value of sample host channels and channels within 5 km of the sample site.

limited range of catchment erosion rates (0.05–0.1 m/ka), this result is consistent with previous studies suggesting positive correlation between erosion rate and channel gradient in an adjusted landscape [e.g., *Kirby and Whipple*, 2001; *Snyder et al.*, 2000; *Wobus et al.*, 2006c]. Moreover, the systematic relationship between channel steepness and erosion rate bolsters the argument that channel gradients upstream of knickpoints are likely adjusted to spatial variations in erosion rate. The range of observed fluvial incision rates also show a positive correlation to channel k_{sn} values, but do not overlap with the range of catchment erosion rates.

[44] The positive correlation between k_{sn} and fluvial incision/catchment erosion rates allows for a brief discussion of the controls on the distribution of fluvial incision rates above channel knickpoints. The spatial variations of tributary k_{sn} across the Anyemaqen Shan occur all within flysch of the Songpan-Garze terrane, and do not correspond directly to mapped plutons. Potential causes for the increase in k_{sn} values toward the core of the range include differential uplift in the Anyemaqen Shan, broad-scale spatial variations in bedrock erodibility, and orographically driven precipitation per unit area. Of these, bedrock variability is unlikely because, with the exception of the restricted outcrops of intrusive bodies and Tertiary sedimentary basins, no regional-scale variation is outwardly apparent in bedrock character across the Anyemaqen Shan. Orographically driven differences in precipitation appear unlikely because this effect would be expected to decrease channel slopes toward the higher-relief portions of the range under a stream power condition, as greater precipitation would increase discharge per unit catchment area.

[45] As a result, we suggest that the landscape above knickpoints in the Anyemaqen Shan approximates a steady state condition, balanced against relatively slow rates of differential rock uplift (probably <0.1 mm/yr), and that channel gradients are balanced with more rapid rock uplift at the center of the range. This result agrees with previous work that associates high topography and steep rivers with high erosion and uplift rates [e.g., *Kirby et al.*, 2003; *Koons*, 1989; *Pazzaglia and Brandon*, 2001]. Larger channels that flow across the interpreted gradient in uplift rate could be expected to show correlative changes in profile form. The apparent steady state form of the above knickpoint landscape implies that these uplift conditions, although slow, have been active for a significant time prior to the introduction of the wave of increased fluvial incision observed in the northern Anyemaqen Shan.

[46] Although the relationship between channel steepness (k_{sn}) and erosion rate appears to be linear over the limited range of erosion rates we sampled (Figure 9), comparison to incision rates and channel gradients from below knickpoints reveals a highly nonlinear relation (Figure 9). Although we recognize the difficulties inherent in comparing two different measures of erosion in a landscape, we think that this relation may be explained in one of two ways. First, the nonlinearity may arise as a consequence of incomplete adjustment of channel profiles to base-level fall. This would imply a relatively long timescale (>100 ka) for gradient adjustment, perhaps more consistent with transport-limited models of incision [*Whipple and Tucker*, 2002]. On the other hand, similar nonlinear relationships between channel steepness and erosion rate have been observed in eastern Tibet [*Ouimet et al.*, 2006] and in coastal California [*Duvall et al.*, 2004; *Snyder et al.*, 2003], and may reflect thresholds in erosion process and/or adjustments in channel hydraulic geometry.

6.3. Reconstructing Channel Profiles

[47] We utilize the assumption of steady state channel gradients to reconstruct the relief on channel profiles prior to the onset of rapid incision along the Yellow River. We project the slope-area array of the channel upstream of the knickpoint to its junction with the Yellow River and predict the elevation drop between the knickpoint and the tributary junction (Figure 10). Reconstructed channel profiles are calculated on the basis of the k_{sn} values of tributary reaches above knickpoints, a reference concavity of 0.42, and the cumulative upstream drainage area along a channel. Channel gradients were calculated at 0.5 km intervals along channel reaches below knickpoints and integrated along the length of the channel to reconstruct paleochannel elevations downstream of the modern knickpoint elevation. To determine minimum and maximum elevation bounds on the reconstructed junction elevation, we combine the uncertainties on k_{sn} values upstream of knickpoints with the uncertainties on knickpoint elevation to derive maximum and minimum estimates of junction elevation.

[48] Comparison of reconstructed elevations of the tributary junctions with field-based estimates derived from the presence of strath terraces in two tributaries allow a limited test of the validity of this method of reconstructing former channel profiles. As described above, modern floodplains along two major tributaries, the Zhe Qu and Sai Qe, grade into continuous strath terraces that extend to the junction with the Yellow River (Figures 10a and 10b). This relationship suggests that the terrace reflects the progressive abandonment of a previous channel floor during knickpoint migration. Along Zhe Qu, strath terraces first appear along the channel just downstream of the knickpoint identified via

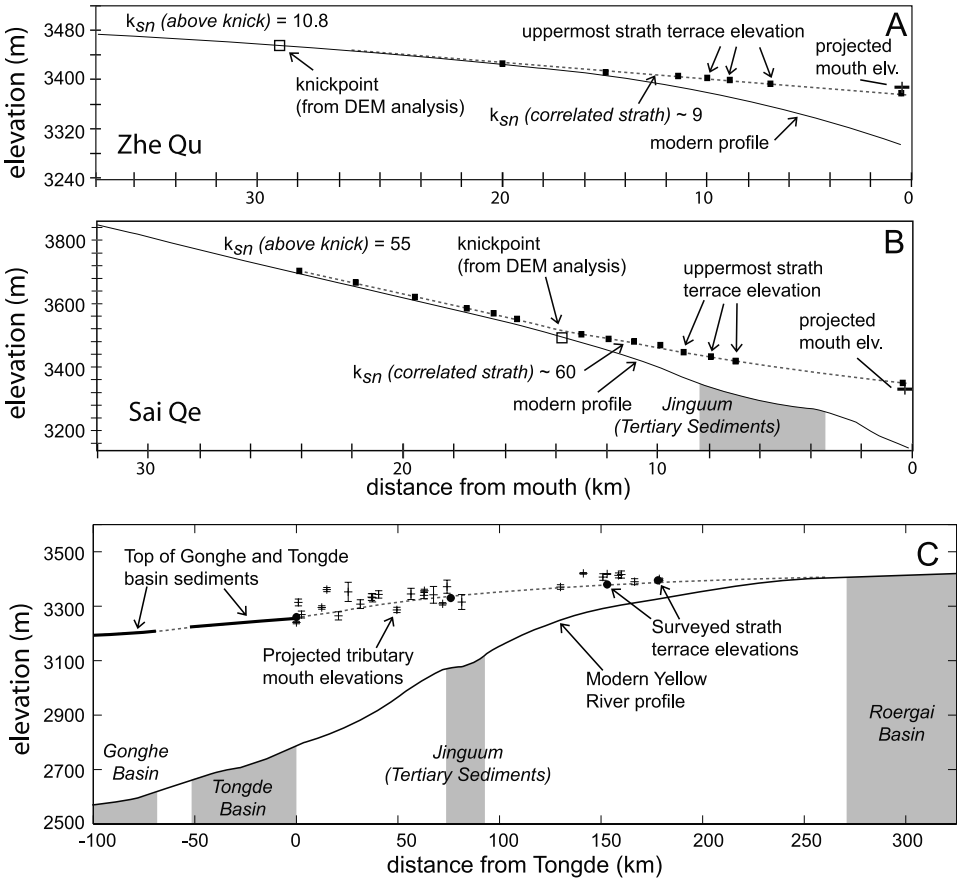

Figure 10. (a and b) Longitudinal profiles along the lower reaches of Zhe Qu and Sai Qe, respectively, displaying the locations of the knickpoint identified via DEM analysis; surveyed uppermost strath terrace elevations; and the projected, preincisional wave elevation of the tributary mouth based on channel θ and k_{sn} values upstream of the knickpoint. The limits of tertiary sedimentary basin bedrock associated with the Jinguum basin are shaded along Sai Qe. The change in channel gradient across the basin is related to lithologic contrast and is not interpreted as a knickpoint in this analysis. (c) Modern and reconstructed preincisional wave longitudinal profiles of the Yellow River between the Roergai and Tongde basins. Profile reconstruction is based on consideration of strath elevations, projected tributary mouth elevations, and the top of fill in the Tongde and Gonghe basins; see text for further discussion.

DEM analysis (Figure 10a). The height of the uppermost strath along Zhe Qu above the modern channel continues to grow until attaining an elevation of ~65 m at the Yellow River junction (corresponding to ~3365 m asl). Along Sai Qe, a broad, uppermost strath surface is present ~3–4 m above the modern channel upstream of the identified knickpoint (Figure 10b). Downstream of the knickpoint, however, the elevation of this uppermost strath gradually climbs above the channel to attain a height of ~220 m at the Yellow River junction (~3340 m asl). The uppermost terrace elevations along both tributaries roughly define channel profile with a k_{sn} value that is similar to that observed in the modern channel above the knickpoints. On the basis of these observations, we consider uppermost strath terraces elevations along Zhe Qu and Sai Qe to represent the quasi–steady state channel form of those tributaries prior to onset of rapid incision rates associated with base-level fall.

[49] Comparison of the elevation of strath terraces at or near the junction of these tributaries and the Yellow River with reconstructed profiles using the method described above provides an internal test of consistency of the method. At the mouth of Zhe Qu, the measured strath elevation of ~3365 is within error of the projected paleochannel mouth elevation of 3368 ± 10 m (Figure 10a). Similarly, a strath at the mouth of Sai Qe of ~3340 is just outside of the error bounds of the projected paleochannel elevation mouth of 3331 ± 7 m. Although the elevations of terraces may have been influenced by differential rock uplift since abandonment, our estimates of the timing of incision and background rock uplift suggest that this is probably a minor addition to the uncertainty (<8 m). Moreover, the consistency between strath elevations and the projected initial channel profile appears to validate our use of tributary profiles to reconstruct former positions of tributary junctions along the Yellow River.

[50] Overall, we utilized 30 tributaries along the Yellow River between the Roergai and Tongde basins to reconstruct the shape of the former Yellow River profile (Figure 10c). These reconstructed elevations are similar to the highest strath surfaces we observed along this reach of the river. Moreover, elevations define a trend that intersects the tops

of fill in both the Tongde and Gonghe basins. This reconstructed profile reveals a relatively low-gradient channel that was apparently graded to the sedimentary fill within the basins downstream of the northern Anyemaqen Shan prior to the onset of rapid incision. Interestingly, former channel gradients appear to be somewhat steeper within the Anyemaqen Shan relative to gradients within the basins both upstream and downstream (Figure 10c). To test this, we calculated k_{sn} values as a function of position along the reconstructed profile and find that they are similar in magnitude and distribution to the modern k_{sn} values observed upstream of knickpoints in adjacent tributaries (Figure 8). This result is internally consistent, in that it implies that both the Yellow River and its tributaries were graded to a spatially variable forcing across the Anyemaqen Shan. Moreover, the fact that the paleo–Yellow River profile appears to have been graded to thick fluvial deposits in the Tongde basin implies that this basin acted as a local base level for the northern Anyemaqen Shan.

7. Discussion and Implications

[51] Channel profiles of the Yellow River and its tributaries downstream of the Roergai Basin all exhibit a downstream increase in channel gradient consistent with models of transient profile adjustment to an increase in rock uplift rate (or base level fall) [e.g., *Whipple*, 2001]. Our incision rate data confirms this interpretation and indicates that the lower reaches of the Yellow River are characterized by incision rates on the order of 1–2 mm/yr, while tributary reaches upstream of knickpoints are incising at much slower rates (0.05–0.1 mm/yr). In this field site, we interpret the observed knickpoints to mark a transient boundary between channels extents adjusted to an older, lower incision rate, and those adjusted or adjusting to a newer, higher incision rate. The upstream migration of this boundary is apparent along large tributaries, where it is possible to trace a continuous strath surface upstream to its junction with the active channel floor (Figures 3 and 10). Here we consider the implications of these rates and patterns of transient incision and river profile evolution in the Anyemaqen Shan from both a process-based perspective of the controls on the rate and form of transient channel response and a regional perspective of the driving mechanisms for channel incision.

7.1. Exhumation of the Tongde Basin and the Onset of Transient Incision

[52] The marked increase in fluvial incision rate associated with the observed knickpoints in the northern Anyemaqen Shan could be in response to either 1.) a large magnitude step change in rock uplift rates across the entire Anyemaqen Shan or 2.) a drop in relative base level along the Yellow River downstream of the range. Our reconstruction of the former profile of the Yellow River suggests that it was graded to the top of fill in the Gonghe and Tongde basins. This implies that the onset of rapid incision along the Yellow River in the northern Anyemaqen Shan is part of the same event that led to the abandonment and exhumation of these basins. Given that basins downstream of Gonghe have also been recently incised by the Yellow River [e.g., *Li et al.*, 1997; *Metivier et al.*, 1998], it seems unlikely that the entire northeastern corner of the Tibetan Plateau experienced a uniform pulse of rock uplift. Rather, it seems likely that a wave of incision was initiated from some location downstream of these basins and has subsequently propagated up the Yellow River. A full exploration of the causes of this incision is beyond the scope of this paper, and will require extensive investigation of the timing of both basin fill and excavation along the course of the Yellow River.

7.2. Tributary Response to Transient Incision

[53] The distribution of knickpoints within the Yellow River catchment provide an opportunity to characterize the evolution of this transient fluvial system. The presence of knickpoints at uniform elevations throughout the watershed is, to first order, consistent with simple models of knickpoint migration [e.g., *Niemann et al.*, 2001]. However, channel profiles downstream of knickpoints exhibit convex profiles that may be indicative of a somewhat more complicated response. These observations motivate an analysis of whether simple models of fluvial incision can capture both aspects of channel response.

7.2.1. Knickpoint Vertical Celerity

[54] One of the most remarkable results of our analysis is the relative uniformity of knickpoint elevations throughout the northern Anyemaqen Shan (Figure 6). Accounting for the allowable errors in determined knickpoint elevations, 81% of knickpoints fall within 25m of the population mean of 3430 m. If the subtle upstream increasing trend in knickpoint elevations is considered along with the range of allowable errors, then 85% of knickpoints fall within 25 m of the trend. Interestingly, the top of the steep portion of the Yellow River (~3410 m) falls within this range of observed knickpoint elevations, suggesting that both trunk stream and tributaries are responding at similar rates. Moreover, we observe no dependence of knickpoint elevation on drainage area despite a wide range of tributary sizes analyzed (Figure 5). As noted above, the horizontal position of knickpoints does show a power law dependence on drainage area. These observations lead us to infer that the uniform elevation distribution of knickpoints reflects, at least to first order, a constant vertical celerity of knickpoints throughout the channel network, consistent with the migration of knickpoints as a kinematic wave.

7.2.2. Modeling of Channel Response

[55] To test whether a simple model of fluvial incision can capture the response of tributaries in this landscape to base-level fall, we utilize numerical solutions to a stream power type incision rule [*Whipple and Tucker*, 1999] to model transient channel profile evolution. Details of the model are provided in the supplementary data. We focus only on the tributaries Zhe Qu and Sai Qe, as our field work on strath terraces along these drainages provides constraints on initial profile form and the timing and rate of incision. Our approach is to vary model parameters and ask what combinations can match profiles and erosion rates both upstream and downstream of knickpoints. We emphasize that our analysis is illustrative only; we do not perform a comprehensive search of parameter space [e.g., *Tomkin et al.*, 2003]. Rather, we focus on representative models of erosion by boundary shear stress ($n \sim 0.6$ in equation (2); see also the supplementary data), unit stream power ($n \sim 1$), and a somewhat more nonlinear rule ($n \sim 1.2$, perhaps representative of incision dominated by abrasion, [*Whipple*

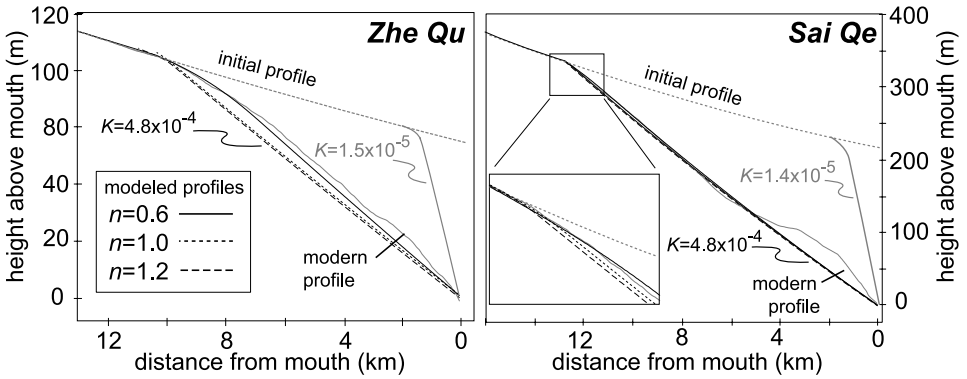

Figure 11. Profile modeling results compared to the below knickpoint extents of Zhe Qu and Sai Qe. Modern tributary profiles are labeled, and the initial condition profiles are shown in gray. The profiles modeled by adjusting K values to fit field incision and chronology constraints are shown for the three chosen values of n. K values corresponding to the $n = 0.6$ profiles are shown in black. For reference, the results of the model run with $n = 0.6$ and the K value used to describe the steady state profile are shown in gray.

et al., 2000]). Model results are compared to channel profiles and incision rates (Figure 11).

[56] A series of initial condition model profiles were first constructed to fit to the profile forms above knickpoints in both Sai Qe and Zhe Qu under the assumption that these profiles represent a quasi-equilibrium condition adjusted to balance erosion rates. These initial profiles were constructed using the "best fit" concavity from the whole of the data ($\theta = 0.42$) and a range of values for n (see above). We determined the value of the erosion coefficient (K) for each n by assuming that profile steepness was adjusted to match erosion rate of 30m/Ma (equivalent to the ^{10}Be determined erosion rates above knickpoints). Importantly, the upstream profiles of Sai Qe and Zhe Qu are well described by very similar sets of K values for each value of n (Table 4).

[57] We subject these initial profiles to a base-level fall at the boundary of the model that is prescribed at a rate and duration that match the chronologic constraints from fluvial terraces (see above). At Sai Qe, these constraints suggest ~220 m of incision in ~100 ka, whereas at Zhe Qu they suggest ~65 m of incision in ~30 ka. We maintain background rock uplift rates of 0.03 m/ka in all model runs. We find from these experiments that we cannot match the degree of knickpoint retreat for any value of n with the erosion coefficients (K) determined from the steady state profile (Figure 11 and Table 4). In all cases, the modeled knickpoints propagate only a fraction of the distance that has been transited by the actual knickpoints (Figure 11). This first-order result suggests that, if a stream power type model is representative of channel response, transient incision must involve some adjustment in erosion coefficient (K). The exact nature of this adjustment remains to be determined, but may reflect thresholds in the incision process [e.g., *Snyder et al.*, 2003] and/or adjustments in channel width [e.g., *Duvall et al.*, 2004; *Finnegan et al.*, 2005; *Wobus et al.*, 2006b].

Table 4. Profile Forward Modeling Results

Zhe Qu						
n	m/n	K	U, m/ka	BL, m/ka	Run Time, ka	RMS Error
Fit to Profile Above Knickpoint						
0.6	0.42	1.38×10^{-5} ($m^{0.16}$)/yr	0.03	0.08	800	5.76
1	0.42	3.7×10^{-6} ($m^{0.5}$)/yr	0.03	0.086	750	21.94
1.2	0.42	1.9×10^{-6} ($m^{-0.01}$)/yr	0.03	0.13	500	26.56
Fit to Profile Below Knickpoint						
0.6	0.42	4.8×10^{-4} ($m^{0.16}$)/yr	0.03	2.16	30	2.42
1	0.42	9.5×10^{-5} ($m^{0.5}$)/yr	0.03	2.16	30	5.43
1.2	0.42	4.1×10^{-6} ($m^{-0.01}$)/yr	0.03	2.16	30	5.19
Sai Qe						
n	m/n	K	U, m/ka	BL, m/ka	Run Time, ka	RMS Error
Fit to Profile Above Knickpoint						
0.6	0.42	1.5×10^{-5} ($m^{0.16}$)/yr	0.03	0.05	4100	13.04
1	0.42	4.0×10^{-6} ($m^{0.5}$)/yr	0.03	0.13	1750	14.68
1.2	0.42	2.2×10^{-6} ($m^{-0.01}$)/yr	0.03	0.21	1025	15
Fit to Profile Below Knickpoint						
0.6	0.42	4.8×10^{-4} ($m^{0.16}$)/yr	0.03	2.2	100	11.37
1	0.42	6.5×10^{-5} ($m^{0.5}$)/yr	0.03	2.2	100	12.107
1.2	0.42	3.5×10^{-6} ($m^{-0.01}$)/yr	0.03	2.2	100	12.2

[58] In a second series of models, we adjust the erosion coefficient (K) to generate profiles that match the degree of knickpoint retreat during incision. In these simulations, best fit K values were chosen for each n value that allowed the location of the modeled knickpoints to correspond to the location of the actual knickpoints in Sai Qe and Zhe Qu ($\sim$12.5 and 10.5 km upstream, respectively (Figure 11)). One interesting result of this analysis is that the resultant "best fit" values for K (for a given value of n) are very similar between the two tributaries (Table 4), suggesting a similar response between the two systems.

[59] From these results, we can evaluate whether the profile is best fit by a given dependence of erosion rate on channel gradient. Previous work has demonstrated that the shape of the profile immediately downstream of knickpoints should depend on the relationship between incision rate and channel gradient (n in equation (2)) [*Tucker and Whipple*, 2002]. For each value of n, a total RMS error between the modeled and observed profile form was constructed to evaluate goodness of fit along the length of the channel between the knickpoint and the Yellow River. In both of the modeled tributaries, the broad convex form of the observed knickpoints result in the lowest RMS error values for profiles modeled using an $n = 0.6$. The various model profiles are only subtly different from one another, however, resulting in relatively small differences in RMS error values. In Sai Qe, a mapped lithologic variation over 2–5 km upstream of the tributary mouth results in a poor model fit to this lower portion of the profile and high RMS errors for all values of n (Figure 11). Thus, although we cannot definitively assess which of these incision models best capture transient channel profile evolution, it appears that the broad convex profiles downstream of knickpoints require a value of $n < 1$ in a stream power type rule.

7.2.3. Complex Transient Channel Response

[60] The spatial pattern of channel steepness indices below knickpoints in the northern Anyemaqen Shan lends further insight into the manner of channel response to increased incision rates. Three aspects of our results suggest that channel gradients downstream of knickpoints may be incompletely adjusted to relative changes in base level during excavation of the Tongde basin: First, most profiles are similar to those of the Zhe Qu (Figure 3) in that they display a broad convex reach downstream of knickpoints characterized by systematically increasing k_{sn} values as they approach the Yellow River. We do not observe a transition back to a concave-up profile that one might attribute to a new steady state condition. Rather, it seems likely that these channels have not yet completely adjusted to the increase in incision rates. Second, a comparison of k_{sn} values from channels downstream of knickpoints with those determined upstream (Figure 9, inset) reveals a strongly nonlinear relationship between steepness indices and erosion rates. As discussed above, such a relation can arise in steady state channels, as a consequence of thresholds in incision or adjustments in channel width, we find it likely that this relationship reflects, in part, an incomplete adjustment of channel gradients downstream of knickpoints. Third, the spatial pattern of k_{sn} values below knickpoints (Figure 8a) also implies either a significant variation in incision rates, reaching a maximum $\sim$50 km upstream from Tongde, or incomplete adjustment of channel profiles to the wave of incision. Given the profile shapes, we consider the latter explanation more likely and suggest that gradients downstream of the knickpoints may be responding to the transient increase in sediment flux engendered by the wave of incision [*Sklar and Dietrich*, 1998].

7.2.4. Implications for Channel Incision Models

[61] Our results are intriguing in that they suggest that some aspects of simple models for fluvial incision and knickpoint migration are consistent with channel response in this landscape while others are not. In particular, the dependence of knickpoint position on drainage area, and the independence of knickpoint elevation, suggests that the celerity of knickpoints may adequately captured by a power law relationship between S and A. Our results thus imply that the migration of the upstream limit of transient channel steepening in the Anyemaqen Shan migrates as a kinematic wave [cf. *Stock et al.*, 2005].

[62] In contrast, the response of channel gradients downstream of knickpoints does not appear consistent with a simple detachment-limited model of transient channel adjustment. Although the broad increase in channel gradients can be reproduced by a detachment-limited model with $n < 1$, this result requires that the erosion coefficient, K, must adjust between the relict and transient parts of the channel. This implies a difference in the processes that control the erosional efficiency described by K between the low- and high-gradient channel reaches that is not adequately captured in the stream power type models. The fact that the same sets of K values can describe the Sai Qe and Zhe Qu profiles suggests that this dependence of erosional process on gradient is consistent between the two tributaries, and may be across the rest of the channel network.

[63] Channel convexities observed below knickpoints are also qualitatively similar to the predictions of incision models that explicitly consider a role for sediment flux in modulating channel incision [e.g., *Sklar and Dietrich*, 1998; *Whipple and Tucker*, 2002]. Although we cannot fully evaluate these models in this landscape, it is possible that they may capture both the apparent propagation of knickpoints as a kinematic wave and the apparent incomplete adjustment of channel gradients downstream of knickpoints. Additionally, the spatial pattern of steepness indices downstream of knickpoints (Figure 8a) could be interpreted to reflect the temporal evolution of channel gradients following knickpoint passage. We caution that the spatial variations in erosion rate upstream of knickpoints makes this assumption tentative. Nonetheless, it is possible that the maximum in k_{sn} values observed $\sim$50 km upstream of the Tongde basin might reflect "oversteepening" of channel gradients in response to increased sediment delivery in the wake of knickpoint passage. Similar behavior is observed in numerical implementation of a sediment flux–dependent model of fluvial incision [*Gasparini et al.*, 2006] although we acknowledge the need for improved characterization of channel steepnesses below knickpoints and information on sediment grain size and caliber in order to test this hypothesis.

7.3. Implications for Active Tectonism in the Northeastern Tibetan Plateau

[64] Our results also carry implications for active deformation of the lithosphere in northeastern Tibet. As argued above, channel profiles and erosion rates upstream of

knickpoints reveal a landscape of subdued relief and slow erosion rates that we interpret to be adjusted to balance rock uplift rates across the Anyemaqen Shan. Covariations in erosion rate and channel steepness suggest that differential rock uplift is occurring in a broad, domal pattern across the range. Erosion rates appear to be approximately 2 times faster in the central part of the range relative to the northern and eastern peripheries, although the overall rates appear to be quite slow relative to subsequent incision along the Yellow River. The fact that reconstructed gradients along the Yellow River trunk stream appear to increase toward the center of the range, matching variations in tributary k_{sn} patterns, is consistent with our inference of a landscape adjusted to the prevailing pattern of tectonic forcing. Attainment of a steady state condition suggests that this deformation field has been relatively stable for a significant period of time, probably >500 ka (the inferred onset of incision in the Tongde basin). Thus our results support the hypothesis that high topography in the Anyemaqen Shan reflects, in some part, deformation associated with the tip of the Kunlun fault [*Kirby et al.*, 2007]. The broad wavelength of this deformation implies that the high topography of the Anyemaqen Shan is either supported elastically by a strong upper crust or maintained by distributed shortening above a weak crustal layer. Evaluation of these competing mechanisms, however, will require a more comprehensive investigation of the active deformation field and crustal rheology.

[65] As noted above, the driving mechanisms for regional fluvial incision along the Yellow River are also not well understood. Our results characterize the upstream extent of transient incision along the course of the river, and, together with constraints on the onset of incision at the margin of the plateau (ca. 1.7 Ma [*Li et al.*, 1997]), suggest that the wave of incision has migrated ~500 km upstream (Figure 1) since this time. Whether incision propagated at a constant rate or whether it was modulated by active faults and/or lithologically resistant sills in the Gonghe and Guide basins (Figure 1) remains unknown. Moreover, whether the ultimate cause of incision was a drainage capture across the plateau margin or whether incision reflects long-term elevation changes of the plateau surface remains an outstanding question that will require additional records of the time-space patterns of incision along the river course.

8. Conclusions

[66] Topographic analysis of channel profiles in the Anyemaqen Shan reveals a distinct transient wave of fluvial incision in the headwater regions of the Yellow River. Tributary channels characterized by broad downstream increases in channel gradient, resulting in convex-up profiles, are present throughout the range upstream of a deeply incised Tertiary basin. Upstream of knickpoints, erosion rates determined from ^{10}Be inventories in modern sediment are slow (0.05–0.1 m/ka), but vary systematically with channel steepness. Reconstruction of the former profile of the Yellow River from tributary profiles and field observations of strath terraces reveals similar variations in channel steepness along the profile that we interpret to reflect variations in rock uplift rate across the range. Transient incision associated with basin excavation is superimposed upon these variations in channel steepness at significantly higher rates (~1–2 m/ka). The upstream limit of steep reaches associated with this incision occurs at nearly uniform elevations throughout the watershed, consistent with behavior expected from a detachment-limited model of fluvial incision. However, the rate of knickpoint migration, and the shape of channel profiles can only be explained by a simple, stream power type model if the erosional efficiency of the channel increases with incision rate and if the exponent on slope (n) is less than unity. Moreover, spatial variations in channel steepness downstream of knickpoints suggest that gradient adjustment following the wave of incision may be modulated by increases in sediment load. Our results thus identify a significant incisional event along one of the major Tibetan drainages, delineate a broad region of differential rock uplift in the northeast Tibetan plateau, and highlight the utility of channel profile analysis to explore the range of transient channel response to changes in external forcing.

Appendix A: Integral Method and Uncertainties on Channel Steepness (k_s)

[67] As described in the text, the development of the data handling methods employed here were driven by the need to reduce scatter in raw pixel-to-pixel slope estimates from digital elevation models [*Wobus et al.*, 2006c]. The large degree of scatter present in pixel-to-pixel estimates of channel gradient stems from relatively minor noise in the longitudinal profiles extracted from DEMs; taking the spatial derivative exaggerates this noise. Efforts to smooth the gradient data usually involve a combination of the following: subsampling the long profile, fitting piecewise linear regressions to the long profile to estimate local slope, applying a moving-average filter to profile elevations, and taking binned averages of $\log S - \log A$ [cf. *Wobus et al.*, 2006c]. A viable alternative to these methods was proposed by *Royden et al.* [2000]. Instead of differentiating the long profile to derive an estimate of S, one can integrate both sides of equation (1) to write

$$z(x) = k_s \int_0^x A(x')^{-\theta} dx' \equiv k_s \chi(x)$$

[68] The transformed variable $\chi(x)$ can be determined directly from drainage area data by simple numerical integration. That is, the method requires no assumptions about Hack's law. Herein we refer to this method as the integral method of determining channel steepness.

[69] Segments of the channel profile that are well described by a concavity index equal in value to θ will be linear on plots of z versus χ (Figure 3, bottom plot). The slope of the line is k_s. Segments of the channel profile that are either (1) not well described by a power law relation between local slope and upstream drainage area, or (2) exhibit a concavity index different from θ, will be curved. Thus standard linear regression of z versus χ can be used to (1) evaluate the degree of linearity by evaluating correlated residuals, and (2) estimate k_s (K. Whipple, personal communication, 2006). We exploit the latter to derive estimates of the uncertainty on values of k_s, simply from the uncertainty in the slope of the regression [*Bevington and Robinson*, 1992], implemented in MATLAB. This constitutes the

primary advantage of the integral method. However, as the best fit value of θ is not known a priori; in practice one must either use standard $\log S - \log A$ relations to find θ, or compute $\chi(x)$ for a range of θ values and test for linearity over the channel segment of interest. In our experience this method, and the slope-area methods (as described by *Wobus et al.* [2006c]) yield identical results.

[70] **Acknowledgments.** The authors would like to thank Xuhua Shi, Fan Chun, Erchie Wang, Charlie Angerman, Kym Klein, and Jean Dixon for help in the field and laboratory. Reviews by Itai Haviv, Frank Pazzaglia, and Associate Editor Josh Roering significantly improved the analysis and presentation of data in the manuscript. Interpretation of the cosmogenic data was facilitated by codes developed by Greg Balco. This research was partially supported by NSF grant EAR-0229955 and a NASA GSRP fellowship to Harkins.

References

Anderson, R. S., et al. (2006), Facing reality: Late Cenozoic evolution of smooth peaks, glacially ornamented valleys, and deep river gorges of Colorado's Front Range, in *Tectonics, Climate, and Landscape Evolution*, edited by S. D. Willett, et al., *Spec. Pap. Geol. Soc. Am.*, *398*, 397–418.

Balco, G., and J. O. H. Stone (2005), Measuring middle Pleistocene erosion rates with cosmic-ray-produced nuclides in buried alluvial sediment, Fisher Valley, southeastern Utah, *Earth Surf. Processes Landforms*, *30*, 1051–1067.

Beaumont, C., et al. (1992), Erosional control of active compressional orogens, in *Thrust Tectonics*, edited by K. R. McClay, pp. 1–18, Chapman and Hall, London.

Berlin, M. M., and R. Anderson (2007), Modeling of knickpoint retreat on the Roan Plateau, western Colorado, *J. Geophys. Res.*, *112*, F03S06, doi:10.1029/2006JF000553.

Bevington, P. R., and D. K. Robinson (1992), *Data Reduction and Error Analysis for the Physical Sciences*, 2nd ed., 328 pp., McGraw-Hill, New York.

Bishop, P., T. B. Hoey, J. D. Janson, and I. Lexartza Artza (2005), Knickpoint recession rate and catchment area: The case for uplifted rivers in eastern Scotland, *Earth Surf. Processes Landforms*, *30*, 767–778.

Brown, E. T., et al. (1996), Denudation rates determined from accumulation of in-situ produced ^{10}Be in the Luquillo Experimental Forest, Puerto Rico, *Earth Planet. Sci. Lett.*, *129*, 193–202.

Bruguier, O., et al. (1997), U-Pb dating on single detrital zircon grains from the Triassic Songpan-Ganze flysch (central China): Provenance and tectonic correlations, *Earth Planet. Sci. Lett.*, *152*, 217–231.

Clark, M. K., et al. (2004), Surface uplift, tectonics, and erosion of eastern Tibet from large-scale drainage patterns, *Tectonics*, *23*, TC1006, doi:10.1029/2002TC001402.

Crosby, B. T., and K. X. Whipple (2006), Knickpoint initiation and distribution within fluvial networks: 236 waterfalls in the Waipaoa River, North Island, New Zealand, *Geomorphology*, *82*, 16–38.

Duvall, A., et al. (2004), Tectonic and lithologic controls on bedrock channel profiles in coastal California, *J. Geophys. Res.*, *109*, F03002, doi:10.1029/2003JF000086.

Fairbanks, R. G., P. deMenocal, D. Oppo, and W. Prell (1990), A 1.2 Myr record of mid-depth delta ^{13}C variability in the North Atlantic; implications for ocean circulation and atmospheric CO_2, *Eos Trans. AGU*, *71*(43), Fall Meet. Suppl., Abstract O22E-8.

Finnegan, N. J., et al. (2005), Controls on the channel width of rivers: Implications for modeling of fluvial incision of bedrock, *Geology*, *33*, 229–232.

Flint, J. J. (1974), Stream gradient as a function of order, magnitude, and discharge, *Water Resour. Res.*, *10*, 969–973.

Gardner, T. W. (1983), Experimental study of knickpoint and longitudinal profile evolution in cohesive, homogeneous material, *Geol. Soc. Am. Bull.*, *94*, 664–672.

Gasparini, N. M., G. E. Tucker, and R. L. Bras (2006), Network-scale dynamics of grain-size sorting: Implications for downstream fining, stream-profile concavity, and drainage basin morphology, *Earth Surf. Processes Landforms*, *29*, 401–421.

Gilbert, G. K. (1896), Niagara Falls and their history, in *National Geographic Society: The Physiography of the United States*, pp. 203–236, Am. Book, New York.

Gosse, J. C., and F. M. Phillips (2001), Terrestrial in-situ cosmogenic nuclides: Theory and application, *Quat. Sci. Rev.*, *20*, 1475–1560.

Granger, D. E., et al. (1996), Spatially averaged long-term erosion rates measured from in situ-produced cosmogenic nuclides in alluvial sediment, *J. Geol.*, *104*, 249–257.

Hack, J. T. (1957), Studies of longitudinal stream profiles in Virginia and Maryland, *U.S. Geol. Surv. Prof. Pap.*, *294-B*, 45–97.

Hack, J. T. (1973), Stream profile analysis and stream-gradient index, *J. Res. U. S. Geol. Surv.*, *1*, 421–429.

Holland, W., and G. Pickup (1976), Flume study of knickpoint development in stratified sediment, *Geol. Soc. Am. Bull.*, *87*, 76–82.

Howard, A. D. (1994), A detachment-limited model of drainage basin evolution, *Water Resour. Res.*, *30*, 2261–2285.

Howard, A. D., and G. Kerby (1983), Channel changes in badlands, *Geol. Soc. Am. Bull.*, *94*, 739–752.

Howard, A. D., et al. (1994), Modeling fluvial erosion on regional to continental scales, *J. Geophys. Res.*, *99*, 13,971–13,986.

Humphrey, N. F., and P. L. Heller (1995), Natural oscillations in coupled geomorphic systems: An alternative origin for cyclic sedimentation, *Geology*, *23*, 499–502.

Kirby, E., and K. Whipple (2001), Quantifying differential rock-uplift rates via stream profile analysis, *Geology*, *29*, 415–418.

Kirby, E., K. X. Whipple, W. Tang, and Z. Chen (2003), Distribution of active rock uplift along the eastern margin of the Tibetan Plateau: Inferences from bedrock channel longitudinal profiles, *J. Geophys. Res.*, *108*(B4), 2217, doi:10.1029/2001JB000861.

Kirby, E., N. Harkins, E. Wang, X. Shi, C. Fan, and D. Burbank (2007), Slip rate gradients along the eastern Kunlun fault, *Tectonics*, *26*, TC2010, doi:10.1029/2006TC002033.

Koons, P. O. (1989), The topographic evolution of collisional mountain belts: A numerical look at the Southern Alps, New Zealand, *Am. J. Sci.*, *289*, 1041–1069.

Lague, D., and P. Davy (2003), Constraints on the long-term colluvial erosion law by analyzing slope-area relationships at various tectonic uplift rates in the Siwalik Hills (Nepal), *J. Geophys. Res.*, *108*(B2), 2129, doi:10.1029/2002JB001893.

Lal, D. (1991), Cosmic ray labeling of erosion surfaces: In-situ nuclide production rates and erosion models, *Earth Planet. Sci. Lett.*, *104*, 424–439.

Li, J.-J., et al. (1997), Magnetostratigraphic dating of river terraces: Rapid and intermittent incision by the Yellow River of the northeastern margin of the Tibetan Plateau during the Quaternary, *J. Geophys. Res.*, *102*, 10,121–10,132.

Loget, N., P. Davy, and J. Van Den Driessche (2006), Mesoscale fluvial erosion parameters deduced from modeling the Mediterranean sea level drop during the Messinian (late Miocene), *J. Geophys. Res.*, *111*, F03005, doi:10.1029/2005JF000387.

Mackin, J. H. (1948), Concept of the graded river, *Geol. Soc. Am. Bull.*, *101*, 1373–1388.

Metivier, F., Y. Gaudemer, P. Tapponnier, and B. Meyer (1998), Northeastward growth of the Tibet Plateau deduced from balanced reconstruction of two depositional areas: The Qaidam and Hexi Corridor basins, China, *Tectonics*, *17*, 823–842.

Miller, J. R. (1991), The influence of bedrock geology on knickpoint development and channel-bed degradation along downcutting streams in south-central Indiana, *J. Geol.*, *99*, 591–605.

Moglen, G. E., and R. L. Bras (1995), The effect of spatial heterogeneities on geomorphic expression in a model of basin evolution, *Water Resour. Res.*, *31*, 2613–2623.

Montgomery, D. R., and E. Foufoula-Georgiou (1993), Channel network source representation using digital elevation models, *Water Resour. Res.*, *29*, 1178–1191.

Niemann, J. D., et al. (2001), A quantitative evaluation of Playfair's law and its use in testing long-term stream erosion models, *Earth Surf. Processes Landforms*, *26*, 1317–1332.

Nott, J., et al. (1996), Wearing down, wearing back, and gorge extension in the long-term denudation of a highland mass: Quantitative evidence from the Schoalhaven catchment, southeast Australia, *J. Geol.*, *104*, 224–232.

Ouimet, W., K. Whipple, and D. Granger (2006), Rates and patterns of short-term erosion on the eastern margin of the Tibetan Plateau, a transient landscape, *Eos Trans. AGU*, *87*(52), Fall Meet. Suppl., Abstract H21H-01.

Pazzaglia, F. J., and M. T. Brandon (2001), A fluvial record of long-term steady-state uplift and erosion across the Cascadia Forearc High, western Washington State, *Am. J. Sci.*, *301*, 385–431.

Prescott, J. R., and J. T. Hutton (1994), Cosmic ray contributions to dose rates for luminescence and ESR dating: Large depths and long-term time variations, *Radiat. Measure.*, *23*, 497–500.

Rosenbloom, N. A., and R. S. Anderson (1994), Evolution of the marine terraced landscape, Santa Cruz, California, *J. Geophys. Res.*, *99*, 14,013–14,030.

Royden, L. H., et al. (2000), Evolution of river elevation profiles by bedrock incision: Analytical solutions for transient river profiles related to changing uplift and precipitation rates, *Eos Trans. AGU*, *82*(48), Fall Meet. Suppl., Abstract T62F-09.

Safran, E. B., K. X. Whipple, M. Caffee, P. R. Bierman, R. Aalta, and T. Dunne (2005), Erosion rates driven by channel network incision in the Bolivian Andes, *Earth Surf. Processes Landforms*, *30*, 1007–1024.

Sklar, L., and W. E. Dietrich (1998), River longitudinal profiles and bedrock incision models: Stream power and the influence of sediment supply, in *Rivers Over Rock: Fluvial Processes in Bedrock Channels*, *Geophys. Monogr. Ser.*, vol. 107, edited by K. J. Tinkler and E. E. Wohl, pp. 237–260, AGU, Washington, D. C.

Sklar, L. S., and W. E. Dietrich (2001), Sediment and rock strength control on river incision into bedrock, *Geology*, *29*, 1087–1090.

Sklar, L. S., and W. E. Dietrich (2004), A mechanistic model for river incision into bedrock by saltating bed load, *Water Resour. Res.*, *40*, W06301, doi:10.1029/2003WR002496.

Snyder, N. P., et al. (2000), Landscape response to tectonic forcing: Digital elevation model analysis of stream profiles in the Mendocino triple junction region, northern California, *Geol. Soc. Am. Bull.*, *112*, 1250–1263.

Snyder, N. P., K. X. Whipple, G. E. Tucker, and D. J. Merritts (2003), Importance of a stochastic distribution of floods and erosion thresholds in the bedrock river incision problem, *J. Geophys. Res.*, *108*(B2), 2117, doi:10.1029/2001JB001655.

Stock, J., and W. E. Dietrich (2003), Valley incision by debris flows: Evidence of a topographic signature, *Water Resour. Res.*, *39*(4), 1089, doi:10.1029/2001WR001057.

Stock, J. D., and D. R. Montgomery (1999), Geologic constraints on bedrock river incision using the stream power law, *J. Geophys. Res.*, *104*, 4983–4993.

Stock, J. D., R. S. Anderson, and R. C. Finkel (2005), Field measurements of incision rates following bedrock exposure: Implications for process controls on the long profiles of valleys cut by rivers and debris flow, *Bull. Geol. Soc. Am.*, *117*, 174–194.

Stone, J. O. (2000), Air pressure and cosmogenic isotope production, *J. Geophys. Res.*, *105*, 23,753–23,759.

Stuiver, M., P. J. Reimer, and T. F. Braziunas (1998), High-precision radiocarbon age calibration for terrestrial and marine samples, *Radiocarbon*, *40*(3), 1127–1151.

Tarboton, D. G., R. L. Bras, and I. Rodriguez-Iturbe (1989), Scaling and elevation in river networks, *Water Resour. Res.*, *25*, 2037–2051.

Tomkin, J. H., et al. (2003), Quantitative testing of bedrock incision models for the Clearwater River, NW Washington State, *J. Geophys. Res.*, *108*(B6), 2308, doi:10.1029/2001JB000862.

Tucker, G. E., and R. Slingerland (1997), Drainage basin responses to climate change, *Water Resour. Res.*, *33*, 2031–2047.

Tucker, G. E., and K. X. Whipple (2002), Topographic outcomes predicted by stream erosion models: Sensitivity analysis and intermodel comparison, *J. Geophys. Res.*, *107*(B9), 2179, doi:10.1029/2001JB000162.

van der Beek, P., and P. Bishop (2003), Cenozoic river profile development in the Upper Lachlan catchment (SE Australia) as a test of quantitative fluvial incision models, *J. Geophys. Res.*, *108*(B6), 2309, doi:10.1029/2002JB002125.

Van der Woerd, J., F. J. Ryerson, P. Tapponnier, A.-S. Meriaux, Y. Gaudemer, B. Meyer, R. C. Finkel, M. W. Caffee, Z. Guoguang, and X. Zhiquin (2000), Uniform slip-rate along the Kunlun Fault: Implications for seismic behavior and large-scale tectonics, *Geophys. Res. Lett.*, *27*, 2353–2356.

Wang, S., and B. Xue (1996), The environmental history of the Ruoergai Basin since the middle Pleistocene and the comparative study with that of the Loess Plateau, *Sci. China, Ser. D*, *26*, 323–328.

Weislogel, A. L., G. E. Gehrels, H. Yang, S. A. Graham, E. Z. Chang, and J. L. Wooden (2006), Detrital zircon provenance of the late Triassic Songpan-Ganzi complex: Sedimentary record of collision of the North and South China blocks, *Geology*, *34*, 97–100.

Whipple, K. X. (2001), Fluvial landscape response time: How plausible is steady-state denudation?, *Am. J. Sci.*, *301*, 313–325.

Whipple, K. X. (2004), Bedrock rivers and the geomorphology of active orogens, *Annu. Rev. Earth Planet. Sci.*, *32*, 151–185.

Whipple, K. X., and B. J. Meade (2004), Controls on the strength of coupling among climate, erosion, and deformation in two-sided, frictional orogenic wedges at steady state, *J. Geophys. Res.*, *109*, F01011, doi:10.1029/2003JF000019.

Whipple, K. X., and G. E. Tucker (1999), Dynamics of the stream-power river incision model: Implications for height limits of mountain ranges, landscape response timescales, and research needs, *J. Geophys. Res.*, *104*, 17,661–17,674.

Whipple, K. X., and G. E. Tucker (2002), Implications of sediment-flux-dependent river incision models for landscape evolution, *J. Geophys. Res.*, *107*(B2), 2039, doi:10.1029/2000JB000044.

Whipple, K. X., et al. (2000), River incision into bedrock: Mechanics and relative efficacy of plucking, abrasion, and cavitation, *Geol. Soc. Am. Bull.*, *112*, 490–503.

Willgoose, G., R. L. Bras, and I. Rodriguez-Iturbe (1991), A coupled channel network growth and hillslope evolution model: 1. Theory, *Water Resour. Res.*, *27*, 1671–1684.

Wobus, C. W., et al. (2005), Active out-of-sequence thrust faulting in the central Nepalese Himalaya, *Nature*, *434*, 1008–1011, doi:10.1038/nature03499.

Wobus, C. W., et al. (2006a), Hanging valleys in fluvial systems: Controls on occurrence and implications for landscape evolution, *J. Geophys. Res.*, *111*, F02017, doi:10.1029/2005JF000406.

Wobus, C. W., et al. (2006b), Self-formed bedrock channels, *Geophys. Res. Lett.*, *33*, L18408, doi:10.1029/2006GL027182.

Wobus, C. W., et al. (2006c), Tectonics from topography: Procedures, promise, and pitfalls, in *Tectonics, Climate, and Landscape Evolution*, edited by S. D. Willett, et al., *Spec. Pap. Geol. Soc. Am.*, *398*, 55–74.

Zhang, X., et al. (2001), Trends in Canadian streamflow, *Water Resour. Res.*, *37*, 987–998.

Zhengqian, L., et al. (1991), Geological map of Qinghai-Xizang (Tibet) Plateau and adjacent areas, 86 pp., Chin. Acad. of Geol. Sci., Beijing.

Zhou, D., and S. A. Graham (1996), Songpan-Ganzi complex of the west Qilian Shan as a Triassic remnant ocean basin, in *The Tectonic Evolution of Asia*, edited by A. Yin and T. M. Harrison, pp. 281–299, Cambridge Univ. Press, Cambridge, U. K.

N. Harkins and E. Kirby, Department of Geosciences, Pennsylvania State University, University Park, PA 16802, USA. (nharkins@geosc.psu.edu)

A. Heimsath, Department of Earth Sciences, Dartmouth College, Hanover, NH 03755, USA.

U. Reiser, School of Earth Sciences, Victoria University of Wellington, PO Box 600, Wellington, New Zealand.

R. Robinson, School of Geography and Geosciences, University of St. Andrews, St. Andrews KY16 9AL, UK.